PHYSICAL CHARACTERIZATION AND ANTIMICROBIAL PROPERTIES OF PVA-CELLULOSE NANOFIBER BASED FILMS

A thesis presented to the Faculty of the Graduate School

University of Missouri

In Partial Fulfillment of the Requirements for the Degree

Master of Science

---

by

FRANCOIS XAVIER NAYIGIZIKI

Dr. Azlin Mustapha, Thesis supervisor

DECEMBER 2016

The undersigned, appointed by the Dean of the Graduate School, have examined the Thesis entitled

PHYSICAL CHARACTERIZATION AND ANTIMICROBIAL PROPERTIES OF PVA-CELLULOSE NANOFIBER-BASED FILMS

Presented by Francois Xavier NAYIGIZIKI

a candidate for the degree of Master of Science,

and hereby certify that, in their opinion, it is worthy of acceptance.

Azlin Mustapha, PHD., Food Science Program

Mengshi Lin, PHD., Food Science Program

Shramik Sengupta., PHD, Department of Agricultural Engineering

DEDICATION

To my Lord and Savior, JESUS CHRIST who reconciled me to the Almighty God

To my wife, Jolly Mukundwa

ACKNOWLEDGMENTS

I would like to thank my academic advisor, Dr. Azlin Mustapha for her patience, generosity and continuous counseling and advices throughout my journey to achieve this degree. I greatly appreciate for her invaluable mentorship and help towards success in this academic program.

I would also like to thank Dr. Mengshi Lin and Dr. Shramik Sengupta for their precious time while serving on my thesis committee with my academic advisor. They are a blessing to me, and therefore referring to the bible verse in the Genesis 12: 3 the Lord promised to bless those who bless us. May the Lord pour His enormous blessing to the Professors who served on my thesis committee.

My special thanks also go to other instructors, Dr Andrew Clarke, Dr V, Dr. Tse and Dr. Phillip Deming for their sacrifice to provide relevant knowledge I needed to attain this level.

I would also like to extend my special appreciations to my colleagues and lab mates, Prashant , Marwa, Yuan, Fanding,Yuejiao, Chenggeer, Whei, Zhilong, Fouad, Yafan, and Lin Li. To have all of you is the blessing to me. God bless you all.

Finally, I wish to also acknowledge my brothers Pavel Bosovik and his family, Boaz Bett and Justine Obwoge for their intimate relations with me in the United States. You have been a blessing to me. I cannot conclude without thanking my lovely wife, Jolly Mukundwa who endured to stay alone while I was studying abroad. I believe and recognize that it was hard to leave her alone for such a long period.

TABLE OF CONTENTS

LIST OF TABLES

LIST OF FIGURES

PHYSICAL CHARACTERIZATION AND ANTIMICROBIAL PROPERTIES OF PVA-CELLULOSE NANOFIBER-BASED FILMS

François Xavier Nayigiziki

Dr. Azlin Mustapha, Thesis supervisor

ABSTRACT

Hybrid biopolymer-based composite films made up of 5% polyvinyl alcohol (PVA), 2.3% cellulose nano fibers (CNFs) and 1% chitosan, 4% glycerol and 0.5% cinnamon or clove essential oils (EOs) were prepared via a solution blending and casting method. Beef cuts inoculated with *Escherichia coli* O157:H7 and un-inoculated ones were wrapped with the films containing 1% chitosan, and others with the films containing 1% chitosan and 0.5% EOs, and then refrigerated at 4^{o}C. Approximately 2 log reductions of bacterial growth of the cocktail mixture of five strains of *E. coli* O157:H7 was observed for chitosan and EO-added films in two replications after 10 days. For shelf-life studies, beef cuts were wrapped with chitosan and EO-added films and refrigerated at 4^{o}C. An average of 1 log reduction of the total counts was observed with either films containing chitosan and those incorporated with EOs after 10 days.

Physical tests of the polymer based-films showed that the tensile strength of the films was decreased with incorporation of 0.5% EOs. The yellowness of these polymer based films was a result of inclusion of chitosan and cinnamon EOs. For SEM-EDS analysis, rough surfaces were revealed on the surface of both kinds of films. However, EO-added films had the bud-like structures their rough surface. With FTIR analysis, only glycerol was detected to be present in the polymer-based composites.

CHAPTER 1

INTRODUCTION

1.1 Need for the research

Plastic materials have long been used for beverage and food packaging. Owing to their excellent mechanical strength and gas barrier properties, plastics demonstrated to be ideal for food packaging applications.

However, there are concerns associated with plastics used for food packaging. The first issue of plastics is their non–biodegradable behavior which results in environmental pollutions. Petroleum and synthetic polymer-derived plastic wastes are not directly decomposed by the action of microorganisms. As a consequence, plastic wastes can accumulate in the landfills and degrade the environment. According to the year 2012 report by the worldwide watch Institute, 32 and 9.6 million tons ended up in the landfills of the United States and Europe, respectively (Gourmelon 2015).

In developing countries, however, improper plastic waste disposal can obstruct the sewage systems or block water drainages of public areas, such as prisons and markets and compromise the environment. In addition, plastic materials can get in the marine environment and be detrimental to aquatic life. In general, it is estimated that every year, approximately 10-20 million tons of plastic wastes end up in the marine environment (Gourmelon 2015).

To address these environmental concerns while promoting environmental protection, certain countries have adopted measures against environmental degradation by plastic packaging materials. For example, the synthesis, sale and use of the non-biodegradable plastic bags in food establishments are nowadays prohibited in Rwanda. In

this country, biodegradable packaging papers are used in the food packaging and trade. Today, Rwanda uses packaging bags fabricated from cloth, paper and other biodegradable materials.

Food quality and safety is the second issue encountered with plastic packaging materials. While serving as food packaging materials, petroleum and synthetic product-derived plastics can release their matrix in the being-packaged food which may possibly interact with food ingredients and induce off-flavor as well as toxicological defects in the food (Kantominas and others (2006). In this case, the sensory attributes and safety of food products may be compromised. Another issue encountered with the plastic packaging materials is their inability to control food pathogens in the packaged food. Nowadays, the most important pathogens in the food industry are *Salmonella*, *Listeria monocytogenes, Staphylococcus aureus* and *Escherichia coli* O157:H7. These pathogens are well known to be associated with a number of food borne disease outbreaks. In the United States, foodborne disease outbreaks cause about 9.4 million illnesses each year (Scallan and others 2011). In the 2014 annual report, the US Center for Disease Control (CDC) reported 864 foodborne disease outbreaks which resulted in 13,246 illnesses, 712 hospitalizations, 21 deaths and 21 food recalls. In this report, 25 multistate outbreaks were surveyed and it was found that four outbreaks were associated with ground beef contamination with Shiga toxin producing *E. coli* O157:H7 and another with *Salmonella* enteritis (Scallan and others 2011).

In the recent past, biodegradable composite materials that consist of a polymeric matrix and a filler material as reinforcement have received much attention as alternatives to petroleum- synthetic product-derived plastics (Aadil and others 2016). Carbon and

glass fibers are examples of synthetic fillers that are added to polymeric materials to improve tensile and thermal properties of the composite materials. However, synthetic nanofillers are claimed to have a negative impact on the environment and make the material recycling difficult. Substituting these synthetic fillers with natural biopolymers, such as cellulose fibers, starch and chitosan, can solve this problem and ensures the biodegradability and thermal properties of composite materials. Another effect of nanofillers in a polymeric matrix is an increased mobility of polymer chains and enhanced flexibility of composites, thereby extending their functional properties, and providing active packaging materials (Flores and others 2013).

Nanocellulose fibers (NCFs), isolated from cellulosic biomass are common and promising nanofillers in the development of composite films. CNFs used in films as potential packaging materials have received increasing attention, especially for food packaging because of their outstanding mechanical and molecule barrier, as well as renewability and biodegradability properties. The reinforcement effect of CNFs in biocomposites is a result of their high surface area, high aspect ratio and good mechanical properties. Thus, these properties made CNFs more popular with a potential for a wide spectrum of applications.

Biodegradable packaging materials incorporated with CNFs can be an alternative to chemical preservatives to maintain the quality and safety of foods. Thermal and non-thermal processing methods involving chemical preservatives in the food industry have long been applied to preserve food over a period of time. However, consumers' perceptions on food preservatives and processed foods led the food research development to be dynamic and innovative. To respond to their needs, more effort has been devoted to

searching for novel ways to minimally process foods that do not involve any artificial chemical preservatives. Among these methods, food packaging materials incorporated with naturally occurring substances such as essential oils (EOs) are believed to exhibit antioxidant and antimicrobial properties.

Plant-derived EOs consists of antimicrobial compounds which inhibit food pathogenic and spoilage species (Radaelli and others 2016). There exists many plant-derived EOs that were recently reported to possess strong inhibitory activities against microorganisms. Due to their flavor compounds, EOs have also long been well-known to impart flavor in foods and beverage. According to Du and others (2011), cinnamaldehyde in cinnamon EOs and carvatriol present in thyme, clove and oregano EOs are Generally Regarded as Safe (GRAS) and have been widely applied to food to impart flavor of bakery products, sweets, ice cream and chewing gum. However, terpenes and phenols in the EOs were reported to only exhibit antimicrobial activity against bacteria and fungi.

1.2 Objectives of the study

In this study, we synthesized biodegradable and antimicrobial polymer-based composite films using poly (vinyl) alcohol (PVA), CNFs, and chitosan incorporated with EOs. First, our study aimed at evaluating the antimicrobial activity of the synthesized films against various food pathogenic strains. Also applying the same films to food, raw beef was used as a food model to determine the efficacy of antimicrobial polymer-based films against *E. coli* O157:H7. Second, the study also performed physical characterization of the polymer-based films using a combination of techniques such as Texture Analyzer (TA), Scanning electron microscopy (SEM), Energy Dispersive X-ray spectroscopy (EDS), and Fourier transform infra-red spectroscopy (FTIR).

CHAPTER 2

LITERATURE REVIEW

2.1 Cellulose and nanocellulose concepts

Cellulose is the most ubiquitous, abundant and renewable biopolymer in nature (Santos and others 2015). It is a linear structural homo-polysaccharide consisting of D-anhydroglucopyranose units bonded together by β-1,4-glycosidic linkages **(**Zeni and others 2015**)**. Cellulose sources include plants, tunicates, algae and bacteria. Plant cellulose pulp obtained by harsh mechanical grinding is enzymatically (Park and others 2010) or chemically and mechanically (Chaker and others 2014) treated to obtain nanometer-sized cellulose fibrils. Cellulose whose fibrils *have* at least one nanometer-scaled (usually <100nm) dimension is termed nanocellulose (Wachala and others 2013). Depending on their sources, dimensions, functional properties and isolation methods, nanocelluloses exist as cellulose nanofibers (CNFs) or microfibrillated cellulose (MFC), cellulose nanocrystals (CNCs) and bacterial nanocellulose (BNC).

2.1.1 Cellulose nanofibers (CNFs)

Cellulose nanofibers (CNFs) are produced from microfibrils essentially isolated from a plant cell wall by breaking down the hierarchical fiber matrix**.** CNFs consist of long and semi-flexible mesh-like microfibril bundles with polydispersed width ranging from 5 to 20 nm (Frone and others 2011). These bundles consist of entangled cellulose fibrils (Amiralian and others 2015) formed as a result of chemical cross-linking reactions due to numerous and strong hydrogen bonding on the cellulose chains. In this case, CNFs is sometimes referred to as microfibrillated cellulose (Sundaran and others 2012). However, the thinnest fibrils of nanofibrillated cellulose or nanofibrillar cellulose (NFC) or nano fibril cellulose (NFC) consist of fibrils with a dimension of 3-10 nm (Kolakovic

and others, 2012). Functional properties of CNFs are unique and related to the structure of their nanofibrils (Wachala and others 2013). CNFs are made up of alternating amorphous and crystalline regions (Taheri and Samyn 2016) and the crystallinity of NFC ranges from 65-95% based botanical source (Brinchi and others, 2013). Other remarkable properties of NFC are that they have extremely significant tensile strength, stiffness and high aspect ratio (length to width [diameter] ratio) and their very low thermal expansion coefficient (Chen and others 2014).

2.1.2 Cellulose nanocrystals

Cellulose nanocrystals (CNCs), also termed cellulose nanowhiskers (CNW), cellulose microcrystals (CMCs) or nanorods**,** consist of rod-like cellulose structures with a relatively low aspect ratio due to their typical width of 2-20 nm and length ranging from 100 nm to several micrometers. Unlike CNFs, CNCs are not flexible and have no amorphous zones. The particles of CNC have crystallinity varying between 54 and 88% crystalline regions (Moon and others 2011). However, this crystalline degree as well as width diversity and shape of the CNC particles are influenced by the botanical source of cellulosic materials and processing conditions (Habibi and others, 2010).

CNC is prepared though acid hydrolysis of amorphous regions of CNFs. Usually, fibers from cellulosic sources, such as cotton, are subject to concentrated sulfuric acid that breaks down the disordered cellulosic bonds in the amorphous regions of CNFs. The surface of the resulting CNC becomes negatively charged due to the sulfate anions introduced by sulfuric acid while hydrolyzing amorphous cellulosic bonds. As a result, the charged surface ensures stability of the CNC suspension due to electrostatic repulsions.

2.1.3 Bacterial nanocellulose

Bacterial nanocellulose (BNC) is extracellularly produced by aerobic bacteria, such as *Gluconacetobacter, Acetobacter*, *Azotobacter* and *Pseudomonas* spp. Even though bacterial cellulose (BC) looks similar to that synthesized by plants, it is more pure than plant cellulose due to the absence of lignin and hemicellulose. In addition, it is highly crystalline (Nakagaito and others 2010) and has a high tensile strength and purity index (Castro and others 2011). In addition, BC presents high water holding capacity and hydrophobicity and very thin network structure (Kazim 2015). The routine synthesis of BC involves aqueous culture media incorporated with glucose, phosphate and oxygen to grow cellulose-producing species. During bacterial replication, a ribbon-like structure which consists of entangled fibrils of nanocellulose is formed (Kazim 2015).

2.2 Isolation of nanocellulose fibers (CNFs)

CNFs are essentially isolated from plant-cellulosic materials, such as wood pulp, crops, such as sisal (Deepa and others 2015) and cotton (Morais and others 2013,) and food crop by-products, such as bagass (Mandel and Chakaberty 2011), rice and rapeseed stalks and corn straw (Chaker and other 2014). The structure of the cell wall of these plant-based cellulosic sources consists of lignin bounded to woody and non woody fibers which connect hemicellulose and cellulose (Spence and others 2010). Since cellulose microfibrils are arranged in bundles and in entangled-structures, they are surrounded by these non-cellulosic components which form the matrix (Xu and others 2014). Several studies on cellulose fibrillation to produce cellulose nanofibers were conducted previously. In the 1980s, mechanical fibrillation of cellulose in different wood pulps to produce cellulose with nanoscale diameters was pioneered by Turbak and others (1983) and Herrick and others (1983). However, their work became unsuccessful due to the high

energy input for mechanical fibrillation of cellulose and the presence of amorphous matrix of lignin and hemicellulose that surrounds cellulose microfibrils (Xu and others 2014). Since then, more research focused on cutting down energy consumption due to mechanical fibrillation by adopting raw material pretreatment methods. In reality, an intensive mechanical treatment is a prerequisite to produce cellulose nanofibrils. However, several studies applied enzymatic (Park and others 2010; Lopez-Rubio and others 2007; Svagan and others 2007) and chemical pretreatments (Santo and others 2007**;** Chaker and others 2014) before mechanical fibrillation of cellulose fibrils to cut down on energy consumption and improve the efficiency of NFC production.

2.2.1 Delignification

As discussed earlier, the presence of lignin in cellulosic biomass reduces the efficiency of cellulose NFC production. Lignin can affect detailed information on spectroscopic characterization of cellulose nanoscale particles (Hubbell and others 2010) if it is not removed prior to mechanical disintegration of cellulose microfibrils. Several studies have utilized alkaline and chemical pretreatments to disrupt the lignin structure of cellulosic biomass. Sodium hydroxide, acetic acid–sodium hypochlorite (NaClO) (Chaker and others 2014) and acid-chlorite (Hubell and Ragauskas 2010) delignification are the common pretreatments used to remove lignin from cellulosic biomass. However, a given delignification method may affect the overall yield of CNFs if combined with other chemical or physical treatments. In addition, alkaline pre-treatments may degrade cellulose and reduce the degree of polymerization (DP) if they are not monitored (Hubell and Ragauskas 2010). In a study by Chaker and others (2014), it was reported that acetic acid/ $NaClO_2$ followed by TEMPO-mediated oxidation was more effective than alkaline (NaOH) delignification as more than 90% yield of CNFs with high overall appreciable

morphological and optical characteristics were produced using mechanical fibrillation. Thus, the DP of cellulose can be greatly minimized due to acid hydrolysis of cellulose during acid-chlorite delignification.

2.2.2 Enzyme pre-treatment

There are a number of cellulases that specifically act upon and hydrolyze bonds in amorphous regions of a cellulose molecule. In NFC production, endoglucanases are utilized to hydrolyze amorphous regions of cellulose chains for easy mechanical disintegration of cellulose microfibrils to nanosized fibrils (Park and others 2010). Using these enzymes at lower concentrations may be effective for successful mechanical disintegration of cellulose fibers to nanofibers. According to Henriksson and others (2007), pretreatment of enzymatic hydrolysis of the cellulose fiber pulp at 0.02% to hydrolyze amorphous regions of cellulose facilitated mechanical fibrillation and maintained integrity of molecular weight and length of nanofibrillated cellulose fibers.

A combination of enzyme pretreatment and mechanical methods during fibrillation of cellulose fibrils was found to reduce energy consumption and provide cellulose nanofibers of high aspect ratio (Paakko and others 2007). In other studies by Lopez-Rubio and others (2007) and Svagan and others (2007), mechanical and enzymatic pre-treatments of plant-derived cellulose pulp were combined to fibrillate cellulose fibers. In their method, energy consumption due to mechanical fibrillation was remarkably reduced following four procedures: increasing cell wall of the pulp for enzyme pre-treatment using Escher-Wayss refiner, treating the pulp using endoglucanase enzyme, refining again and finally passing the pulp through a high pressure microfluidizer.

Enzyme assisted-mechanical fibrillation of cellulose microfibrils can significantly reduce the diameter of cellulose nanofibers while increasing their length and reducing the

degree of polymerization of cellulose molecules. In a research study on CNFs production from cellulose wood pulp, Henriksson and others (2007) compared CNFs produced from unpre-treated, enzyme pretreated and acid-pretreated cellulose microfibrils of the wood pulps which were mechanically fibrillated in a homogenizer. It was shown that endoglucanases selectively hydrolyzed the amorphous regions of cellulose and produced CNFs with higher molecular weight and larger aspect ratios than CNFs produced with acid-assisted mechanical fibrillation method.

2.2.3 Chemical pretreatments

The structure of cellulose chains consists of crystalline and amorphous regions of cellulose in contrast to CNC which have only the crystalline region of cellulose (Hietala and others 2016). Chemical reactions, such as oxidation, can cause amorphous regions of native cellulose molecules to dissolve because they are easily exposed to reacting chemicals. In contrast, the crystalline regions of cellulose are inaccessible to these oxidizing agents, and hence, do not react with them. Once attacked, the crystalline regions separate from the amorphous regions that dissolve due to oxidation reactions.

Several chemical pretreatment methods have been used to loosen the rigidity of cellulose structures and facilitate mechanical disintegration of cellulose micro fibrils into nanosized fibrils. Periodate chlorite oxidation (Liitamatainen 2012; Kekalainen 2014) and TEMPO-mediated oxidation (Chaker and others 2014) are important promising chemical pretreatment methods that were extensively studied in the production of CNFs. The principle underlying these methods is that they decrease the hydrogen bondings by introducing anions on the surface of cellulose and improving the capacity of mechanical fibrillation. In this section, these methods are discussed as promising and extensively studied chemical pretreatments for effective mechanical disintegration of cellulose

microfibrils (CMFs; cellulose fibrils with micrometer scaled diameter before mechanical disintegration to CNFs) to CNFs.

2.2.3.1 Periodate-chlorite oxidation

In CNF production, periodate and chlorite are used as regio-selective and sequential oxidation pretreatment to introduce anionic groups on cellulose surfaces to enhance mechanical fibrillation (Liitamatainen 2012). As the principle, periodate is able to attack and break C2 and C3 bonds in the glucose repeating units and selectively oxidize their adjacent hydroxyl groups of cellulose, forming 2,3–dialdehydehyde groups along the cellulose molecules (Conley and others 2016; Kekalainen 2014; Liitamatainen 2012). Also termed "dialdehyde cellulose", 2-2 dialdehydes can be converted into dialcohols or disulfite groups (Yang and others 2015). Furthermore, dialdehyde celluloses are oxidatively converted to carboxylic groups on cellulose using chlorite.

In a study by Liimatainen and others (2012) and Kekalainen and others (2014), the level of carboxylic content was determined in the chlorite-oxidized CNFs from wood pulp. The results showed that in the presence of an aqueous solution of acetic acid, sodium chlorite oxidized all of the dialdehyde groups to carboxylate along cellulose chains. Therefore, these results demonstrate that aqueous acid medium favors the effective oxidation of dialdehyde groups to dicarboxyl groups by chlorite. Interestingly, the chlorite oxidation in aqueous acid medium condition preserves the degree of polymerization of fibrillated nanocellulose since it prevents beta–alkoxy fragmentation of cellulose due to aldehydes. Since there no aldehydes in the CNF suspension, the resulting CNFs are presumed to be thermally stable due to high carboxylate content which also contributes to high charge density of the CNF and viscosity of the CNF suspension. Moreover, Liimatainen and others (2012) found that chlorite-oxidization cellulose

improves mechanical fibrillation by reducing the number of passes (1-4 passes without clogging the homogenizer) and maintaining the crystallinity of CNFs. However, mass yield, some decline in fiber length and increase in width were strongly associated with increased carboxyl contents. In the study by Liimatainen and others (2012), it was revealed that a high carboxyl content caused dissolution of cellulose. This is presumably due to the dissolved amorphous regions of cellulose after periodate -chlorite oxidation.

2.2.3.2 TEMPO- mediated oxidation

A regioselective mediated oxidation based on 2,2,6,6-tetramethylpiperidine-1-oxyl moiety (TEMPO) was first used by Santo and others (2007) to pretreat native cellulose surfaces before mechanical production of CNFs with a Waring blender (WB). Nowadays, this chemical pretreatment method is more popular and most commonly used to pretreat cellulose fiber pulp in aqueous and mild conditions before mechanical treatment of wood cellulose pulp.

Practically, sodium hypochlorite (NaClO) is added to aqueous cellulose suspensions in the presence of relative amounts of TEMPO and sodium bromide (NaBr) as catalysts (Chaker and others 2014; Santo and others 2007). At pH 9-11 and ambient temperature, TEMPO-mediated oxidation system facilitates mechanical fibrillation of cellulose fibers by converting primary hydroxyl groups of cellulose to carboxylate to modify the surface of native cellulose. It does so by significantly reducing the energy required for mechanical fibrillation while preserving the crystallinity and morphology of CNFs.

The effect of TEMPO-mediated oxidation on mechanical fibrillation of CMF explored in certain studies. In the study by Santo and others (2007), a TEMPO-mediated oxidation (TEMPO/ NaClO/NaBr) system was applied to native cellulose under pH 9-11

at room temperature. There was depolymerization of cellulose which affected the length and flexibility of the produced CNFs. To preserve the degree of polymerization of cellulose, Saito and others (2007) applied the TEMPO-mediated oxidation using $NaClO_2$/NaClO as oxidizing agents at pH 7. Afterwards, individualized CNFs of 5 nm width and 2 μm length were produced using a Waring blender and ultrasound homogenizer.

A similar pre-treatment method in a recent study by Chaker and others (2014) was followed but using two oxidation pretreatments: TEMPO-$NaClO_2$–NaClO and TEMPO-NaBr-NaClO systems at pH 7 and 10, respectively. Then, chemically pretreated cellulose fibers from rice and rapeseed straw and corn stalks were mechanically disintegrated using a high pressure homogenizer (HPH) and Waring blender (WB).

Chaker and others (2014) assessed the effect of TEMPO-mediated oxidation and alkaline or chlorite delignification on energy consumption, optical aspect, morphological characteristics and yield of produced CNFs. It was shown that the $NaClO_2$ lignification and TEMPO-NaBr-NaClO oxidation were the most effective pre-treatments using a Waring blender that consumed the lowest amount of energy. Regarding the optical aspect, the most transparent CNF suspensions were those produced from $NaClO_2$/acetic acid delignified cellulosic pulp that was pretreated with TEMPO-NaBr-NaClO and mechanically disintegrated using a high pressure homogenizer. On the other hand, delignification and pre-treatment oxidation modes were observed to influence the morphology of CNFs. The study revealed that $NaClO_2$–delignification of cellulosic material resulted in CNFs of around 5-8 nm width and mechanical fibrillation of cellulose that was pre-treated with TEMPO-NaClO system resulted in short CNFs at pH 10.

Finally, Chaker and others (2014) evaluated differences in CNF yield among treatments. It was demonstrated that more than 90% yield of CNFs was successfully produced from cellulosic material that was delignified with $NaClO_2$/acetic acid and pre-treated with a TEMPO-NaBr-NaClO oxidation system at pH 10.

2.2.4 Mechanical treatments

After enzymatic or chemical pre-treatments, several intensive mechanical treatments are used to fibrillate CMFs. While pretreatment methods of CMFs are used to make hydroxyl groups accessible and break the hydrogen bonds to increase bonding potential of CNFs, mechanical treatments are essentially used to mechanically disintegrate CMF into CNF particles which will be in nanoscale diameters.

The problem hindering successful mechanical fibrillation of CMFs is that hemicellulose and lignin matrix surround and bind to the CMF bundles in the cell wall (Xu and others 2014). Fortunately, recent studies were conducted on the pretreatment of cellulose pulp using enzymes or chemicals to remove the non-cellulosic components. Using either kind of pretreatment, mechanical disintegration of CMFs to CNFs could reduce energy consumption. In this review, homogenization and micro fluidization (Taheri and Samyn 2016), grinding (Hoeger and others 2013; Nail and others 2014) and cryo-crushing (Siro and Plackett 2010) are discussed as mechanical fibrillation methods that were explored in a number of studies.

2.2.4.1 Homogenization

CNF production by mechanical fibrillation were first introduced in the early 1980s by Herrick and Turbak (Henriksson and others 2007; Hietala and others 2016; Taheri and others 2016) using a Gaulin homogenizer at high pressure and speed. In Herrick and Turback's method, a mixture of 3-10 nm cellulose fibers and their bundles

were produced by repeatedly passing a wood cellulose pulp suspension through a high pressure homogenizer. However, high energy consumption was the main challenge hindering the success of the CNF production. In addition, the pulp suspension flow and homogenization were prevented due to the clogged slit of the homogenizer. This could subsequently take enormous amounts of time to demount and clean the device for continued operation of defibrillating CMFs.

2.2.4.2 Grinding

In a research study by Nechyporchuk and others (2014), a grinder consisting of a disk refiner was used to improve fibrillation of cellulose fiber bundles into nanostructured fibers. In this method, the pulp suspension is fed between a static stone and rotating stone at 1500 rpm which causes disruption of the fiber cell wall structure and hydrogen bonds due to the generated shearing action of grinding stones (Tonol and others 2007). The diameter of the produced CNFs ranged from 20 to 90 nm but this method still consumed considerable high amounts of energy.

Using this method, the impact of grinding treatments on a number of passes and morphology of produced CNFs was previously evaluated by Iwamoto and Nakagaito (2007) while desiring to produce uniformly sized CNFs. It was claimed that at least five passes of wood fiber pulp through the grading device led to fibers having a nanoscaled diameter. The results also demonstrated that one to three passes produced a mixture of micro- and nanosized fibers whereas results of treatments for more than five passing times showed no significant alterations in the morphology of fiber.

Recent development studies on CNF production improved mechanical defibrillation of CMFs using defibrillating machinery equipped with both grinding and homogenizing devices. A gap between these two kinds of refining discs is designed in

such a way that the morphology and size of the fibers are modified to increase the bonding potential (Nakagaito and Yano 2004). As a consequence, this refining step, also called “external fibrillation of fibers”, peels off S1 and P layers and exposes S2 layers of fiber cell wall. The pulp is then forced through a homogenizing device that uses high shearing force to defibrillate cellulose fibers.

Iwamoto Nakagaito and others (2005) compared the effect of grinding treatments to that due to combined homogenization and grinding treatments in relation to the number of passes and morphological aspect of fibers. The high pressure homogenization-treated fibers up to 14 passes consisted of a mixture of particles having 50 nm and 10 nm in diameters. However, 10 passes of grinder treatments of the high pressure homogenization-treated fiber slurry produced fibers having 50-100 nm width. These results showed that uniformly nano-sized fibers were obtained using the combination of high pressure homogenizer and grinder treatments. Thus, grinder treatments were effective to successfully defibrillate wood pulp fibers into nano-structured fibers.

2.2.4.3 Microfluidization

A microfluidizer uses an intensifier pump to feed fibers through a Z-shape chamber that mechanically defibrillates them using shear and impact forces at high pressure (Ropez-Rubio; Ferrer and others 2012). The size of CNFs produced with microfluidization method is more uniform than that of fibers produced using homogenizer. Typically, CNFs produced with this method have a diameter between 20-100 nm and length of several tens of micrometers.

Ferrer and others (2012) studied an impact of passes of micro-sized crystalline cellulose through a microfluidizer on the morphological aspect of CNFs. They found that the fiber aspect ratio increased with 20 passes through a microfluidizer at 137.9 MPa. As

a result, CNFs highly agglomerated due to increased surface area as it was evidenced by detection of higher hydroxyl group contents.

Comparing this method to high pressure homogenization and grinder treatments, it can be deduced that a microfluidizer provides more uniformly sized and shorter nanofibers than a homogenizer which produces smaller CNFs with a smaller surface area with high number of passes. However, CNFs produced with grinder treatments can lead to nanofibers that are morphologically uniform and high aspect ratios but with few passing times of the cellulose pulp in the grinders. Nevertheless, all these methods are associated with high energy energy-consumption if the fiber pulp is not pretreated with methods discussed in 2.1 and 2.2.sections, respectively.

2.3.4.4 Cryocrushing

Cryocrushing is a rarely used defibrillation method in CNF production. It uses liquid nitrogen to freeze cellulose fibers in order to facilitate their release from the fiber cell wall. Ice crystals form and exert pressure on the cell wall, causing it to disintegrate and release cellulose microfibrils with frozen fibers when an impact force is applied to swollen and frozen fibers (Siro and Plackett 2010).

Wang and others (2007) investigated the impact of cryo-crushing with high pressure and energy on the number of passes and aspect ratios of produced CNFs. They claimed that a large extent of fiber defibrillation was analyzed to be between 15-20 passes resulting in nanofibers having a diameter of 30-100 nm with a length of 5 μm. In another study by Alendar and Sain (2008), chemically pre-treated and air dried CMF pulp (2-9 μm in diameter) from wheat straw and soy hulls was cryocrushed and defibrillated in a mortar and pestle. The study revealed that the nanofibers of 30-40 nm width and length of several micrometers were produced using 20 passes and a pressure of 300 bars.

2.3 Functional properties of isolated CNFs

CNFs exhibit certain functional properties which may be affected by the processing methods (Saurabh and others 2016) or nature of the cellulosic source (Sito and others 2006). CNF characterization techniques have been used to determine morphological characteristics, degree of polymerization, crystallinity and film-related properties of CNFs.

2.3.1 Morphological properties

CNFs may display morphological and size changes due to the processing method and cellulose source. Depending on the cellulosic source and processing methods, CNFs exhibit identical morphological characteristics but different widths and lengths (Saito and others 2006). Typical nanofibril dimensions in width are 3-10 nm (Kolakovic and others, 2012) and length is difficult to determine but several studies estimated the length of nanofibrils to be in several micrometers.

As discussed earlier, chemical treatment methods have potential impact on width and length of CNFs. For instance, Chaker and others (2014) and Saito and others (2007) evaluated the effect of TEMPO mediated oxidation and mechanical fibrillation using a Waring blender and homogenizers on the size of CNFs. These studies reported that the width of resulting CNFs were 5-8 nm and 5 nm wide while their lengths were estimated to be 2μm to several micrometers respectively.

Previously, pioneering studies had applied mechanical treatments to produce CNFs and evaluate their impact on morphological aspects of CNFs. In the 1980's, Herrick and Turbak used a Gaulin homogenizer to produce CNFs. The results showed that a mixture of 3-10 nm sized fibers and their un-fibrillated bundles was produced. Another study by Iwamoto and Nakagaito (2005) used a grinder consisting of a refining

and homogenizing device to study the effect these mechanical treatments might have on the size of the resulting fibers. The study found that CNFs consisting of 50-100 nm widths were produced using this method. Another study by Nechyporchuk and others (2014) used a disk refiner to fibrillate CMFs and the results showed that produced CNFs were 20-90 nm wide.

Later, a study by Saito and others (2006) combined a TEMPO oxidation pretreatment and homogenization method to fibrillate cellulose fibers from bleached soft wood pulp and cotton, tunicin and bacterial cellulose. The study found that CNFs from bleached soft wood pulp and cotton had a uniform 3-5 nm width whereas those produced from *Acetobacter xylinum* and tunicates were 50-100 nm and 10-20 nm wide, respectively.

Based on these studies, it is clear that pre-treatments and mechanical processes have an effect on the size of CNFs. In addition, it is worth noting that the source of cellulose fibers, the lignin content and the presence of hemicellulose may have an impact on the aspect ratio of the isolated CNFs.

2.3.2 Degree of polymerization

In CNF production, chemical pretreatments are used to separate cellulose from non-cellulosic components, such as lignin, hemicellulose and extractives. Acid-chlorite or alkaline pretreatments are common delignification methods used to produce pure cellulose, thus making determination of its degree of polymerization possible (Hallac and Ragauskas 2011). The degree of polymerization of CNFs can be determined using a viscosity method (Iwamoto and Nakagaito 2007 and Zimmermann and others 2010).

However, the degree of polymerization of CNFs can be affected during pre-treatment and mechanical treatments of cellulose materials. In a research study by

Zimmerman and others (2010), cellulose in sulfite-treated soft wood pulp had a degree of polymerization value of approximately 2249, and CNFs obtained by mechanical treatments of sulfite soft pulp had a polymerization degree of 825, which was a 63% decrease.

The same study investigated the effect of these treatment methods on wheat straw and beech pulps. The degree of polymerization of resulting CNFs was found to decrease by 48-15%, respectively. This decrease in degree of polymerization of CNFs was correlated with the reduced aspect ratio of the fibrils after fibrillation process. This means that shorter fibrils with constant diameters have a reduced degree of polymerization. Thus, a microfluidizer and homogenization method used in this study to mechanically disintegrate sulfite soft wood, wheat and beech wood pulps greatly affected the degree of polymerization of produced CNFs.

In CNF production, a high degree of polymerization of CNFs is more desirable since it is associated with a high nanofiber tensile strength. In a study by Kim and Jang (2013), it was shown that CNFs consisting of a degree of polymerization value of 2,730 had a corresponding tensile stress of 177 MPa and modulus of elasticity of 11 GPa. This shows that cellulose of higher molecular weight is critical to increasing the mechanical properties of CNFs.

2.3.3 Degree of crystallinity

CMFs consist of both amorphous and crystalline regions (Hietala and others 2016). Therefore, it is important to know the crystallinity degree of CNFs for better understanding of their properties after isolation. A common method for characterizing this property is the X-ray diffraction method (Park and others 2010). This property is dependent on the botanical source and processing conditions (Habibi and others 2010).

Previously, numerous studies evaluated the impact of pretreatments and processing methods on the crystallinity of produced CNFs. In a study by Alemdar and Sain (2008), it was found that the degree of crystallinity of CNFs isolated from wheat and straw and soy hulls to be around 70%. In another study by Zhu and others (2015), it was reported that chemically pretreated coconut palm petioles to remove non cellulosic components were ground and homogenized in 10-15 passes to yield CNFs with 32.2% increase in degree of crystallinity. However, the authors argued that an additional number of passes using grinding and homogenization could reduce this crystallinity index. This is actually in agreement with another study by Iwamoto and others (2007) who claimed that an increase number of passes greatly reduces the degree of crystallinity of CNFs as a result of crystalline structure damage due to high shear forces in a grinder.

2.3.4 Film properties

NCF-based films are prepared by either solvent casting or vacuum filtration techniques. During the film drying process, a CNF-network is formed as a result of inter-fibril hydrogen bonding. Factors that affect film preparation as well as CNF processing conditions may also influence the CNF-based film properties. These properties, as exhibited by cellulose in the films, include water and gas barrier, mechanical and optical properties.

2.3.4. 1 Water and gas barrier properties

The crystalline content of CNFs ranges between 60-95% (Brinchi and others, 2013). Due to this high crystalline content and dense nanofiber network as a result of numerous and strong hydrogen bonding, CNF films are believed to exhibit good water and gas barrier properties (Nail and others 2014).

Gas barrier and tensile properties of CNF-based films may be influenced by CNF processing methods, such as chemical pretreatments. Sirvio and others (2014) compared gas barrier and mechanical properties of TEMPO-oxidation-based nanocellulose films to those exhibited by periodate-based films. They reported that all of the periodate-based nanocellulose films had high tensile strength (130-163 MPa) and modulus (19-22 GPa). In addition, these films showed a low oxygen permeability of 0.12 cm^3 μm m^{-2} day^{-1} kPa^{-1}at 50% RH. Comparing to TEMPO-oxidized nanocellulose films, the periodate-based nanocellulose films had better mechanical and barrier properties. The author concluded that periodate oxidized nanocellulose is an excellent material to use in the synthesis of nanocellulose films with improved properties.

However, CNFs produced from un-pretreated CMFs can be used to produce films with very high gas barrier property. In a study by Syverud and Stenius (2009), it was found that the oxygen transmission rates of CNF films with a thickness of 21 μm were as low as 17 ± 1 ml m^{-2}/day kPa^{-1}. The author claimed that these data are in agreement with those displayed by other best synthetic polymers, such ethylene vinyl alcohol (3-5 ml m^{-2}/day kPa^{-1}) and polyvinylidene chloride coated polyester films (9-15 ml m^{-2}/day^{-1} kPa^{-1}) of approximately the same thickness with respect to oxygen transmission rates.

Thermally treating CNF films may affect the gas barrier property. Sharma and others (2014) treated films with a gas permeability of 0.007 cm^3μm m^{-2} day^{-1} kPa^{-1} at various temperatures to investigate the effect of temperature on gas barrier properties of CNF films. They found that after thermal treatment at 175°C, the oxygen permeability of the CNF films was reduced by 96% compared to the films without heat treatment.

Even though the CNF films have very good oxygen barrier properties to allow them to compete with synthetic polymer-based films, they had been claimed to have very low water vapor barrier or high water vapor transfer rate. Water vapor transmission rates of CNF films were compared to those exhibited by films made from synthetic polymers and petroleum products (Nail and others 2014). It was reported that CNF films exhibited a water vapor transmission rate of 234 g/m^2 day while polyethylene and plasticized polyvinyl chloride based films had 16.8 g/m^2 day and 118.56 g/m^2 day, respectively. This difference can be explained by the high hydroxyl content of CNFs.

Recent studies have used CNFs that underwent treatment to improve their water barrier property. Sharma and others (2014) reported that thermally treating CNF films at 175^oC for 3 h significantly reduced the water vapor permeability by 50% as compared to untreated CNF films. They argued that the improvement in water barrier property was a result of increased hydrophobicity since they found that there was increase in water contact angle and reduction in porosity by heat treatment. Another study by Rodionova and others (2011) revealed that the water vapor transmission rate of pure CNF films (234 $g\ m^{-2}day^{-1}$) decreased to 167 $g\ m^{-2}\ day^{-1}$ by 30 mins of acetylation treatment. The higher hydrophobicity of the film surface was indicated by higher water contact angles. Another study by Minelli and others (2010) demonstrated that films prepared from carboxymethylated CNFs can be used to produce highly homogenous and less porous films than enzyme pretreated CNF-films. The results showed that these films had improved water vapor barrier property below 80% relative humidity.

2.3.4.2 Mechanical properties

A number of studies investigated mechanical or tensile properties of CNF films. Depending on different analytical methods, and raw material and treatments, a wide

range of values were reported. In a study by Fukuzumi and others (2009), TEMPO-oxidized CNFs were used to prepare transparent CNF films using vacuum filtration method. These CNFs were isolated using TEMPO/NaBr/NaClO oxidation and mechanical disintegration methods. In their study, the CNF films prepared from soft wood CNFs had a tensile stress of 233 MPa and modulus of 6.9 GPa, while those prepared from hard wood CNFs had a tensile stress of 222 MPa and modulus of 6.2 GPa. When incorporated with other biopolymers, CNFs were shown to improve the tensile properties of the composites.

In the study by Savadekar and others (2012), CNFs were added to starch films to investigate their effect on mechanical properties of starch films. The results showed that thermosplastic starch films containing 0.4% CNFs resulted in a 46.1% improvement in tensile stress. Beyond this CNF concentration, the tensile strength decreased. In another study by Virtanen and others (2014) modified CNFs were added to polyvinyl alcohol (PVA) to investigate the effect of CNFs on tensile properties of PVA-based films. The authors claimed that pure CNF films had a tensile stress of 122 MPa, while modified films formed more brittle film and broke at lower tensile stress of 83 MPa and tensile strain (% EB) of 5%. This result is in agreement with another study by Savadekar and others (2012) that evaluated the effect of CNF concentration on tensile properties of kappa-carrageenan based films. The tensile properties of kappa-carrageenan–based films incorporating CNFs were improved with CNF concentrations up to 0.4%. Comparing this result to that of kappa-carrageenan films, it was concluded that the bio-nanocomposites containing 0.4% of CNFs displayed a 44% improvement on tensile strength.

2.3.4.3 Optical properties

The extent of fibrillation of fibers can be evaluated using the transparency of the CNF films or suspension because the light is not refracted or reflected at the air-CNF interface when the wavelength of light comes close to the fiber diameter (Hietala and others 2016). In reality, CNF films do not scatter light because their diameter is less than one-tenth of wavelength of the visible light. Because of this optical property, the CNF films are transparent. The film transparency is determined by measuring the film absorbance at 600 nm using a UV spectrophotometer (Siripatrawan and Harte 2010). Fukuzumi and others (2009) prepared two types of 20 μm thick CNF films from TEMPO-oxidized hard and soft wood cellulose fibers and found that the transmittance at 600 nm was 78 and 90%, respectively. Thus, transparency of the films may depend on the source used to isolate the CNFs.

2.4. Biopolymer-based films

Biopolymer-based films are commonly prepared using a solvent casting method which promotes the formation of hydrogen bonds during the film drying process (Cano and others 2015). Biopolymers used to synthesize films are proteins, lipids and polysaccharides, such as starch, alginate, cellulose derivatives and chitosan. Films prepared from polysaccharides and proteins are well-known for improved mechanical and gas barrier properties but poor water vapor barrier properties. Conversely, films prepared from lipids possess good water vapor barrier properties but poor mechanical properties and oxygen permeability (Carpiné and others 2015). Thus, films prepared by combining these ingredients are said to have improved physical properties.

Typically, polysaccharides such as cellulose,starch, alginate, and pullulans are suited for film synthesis. These ingredients may be incorporated together to increase the

tensile strength of resulting films but a plasticizer is incorporated to make them more flexible and facilitate the film preparation process. Due to strong polymer-to-polymer interaction, plasticizers such as glycerol, polyols and sorbitol are added to the film solutions to improve the flexibility of the films (Sanyang and others 2015).

Also, tensile strength of the polymer-based films can be improved with incorporation of CNFs. In the previous sections of this literature, NCFs were reported to possess outstanding mechanical and optical behaviors as well as enhanced water vapor barrier properties. These properties of CNFs in the bio composites were correlated to high surface area, high aspect ratio and good mechanical properties of CNFs.

2.4.1 Antimicrobial activity of biopolymer-based films

Basically biopolymer-based antimicrobial films are prepared from biopolymers incorporated with antimicrobial agents. Bio-based composite materials with antimicrobial properties can be created to control food pathogens. The composite incorporated with antimicrobials are applied to extend the exponential phase of microbes thereby decreasing their growth and number. As a result, the shelf-life of food is extended and the safety as well as quality of food is maintained.

Polymer-based films can be carriers of antimicrobials and be studied for their inhibitory activities against food pathogens. Chitosan, metal nanoparticles and EOs are examples of antimicrobials that were added to polymer-based films in the microbial assays.

Recent studies used chitosan and cellulose-derivative films incorporated with other antimicrobials to evaluate the antimicrobial activity of microbes using an overlay diffusion method. Regiel and others (2012) developed chitosan films incorporated with

silver nanoparticles to control the growth of *S. aureus*. It was found that low molecular chitosan films with 52 mM of silver loading achieved a 4 log reduction in the population of this antibiotic resistant and bio-film forming organism. In another study, Sandaram and others (2016) found that chitosan and CNF composite films exhibited strong antibacterial activity against strains of *E. faecalis, S. aureus* and *L. monocytogenes*.

Other studies introduced silver and zinc oxide nanoparticles as antibacterial agents to polymer-based films to study their effects on the growth of pathogenic microorganisms. Zinc oxide embedded in hydroxypropyl methylcellulose (HPMC) films at 0.04% was also found effective for inhibiting the growth of *A. hydrophila, B. subtilis, E. coli, P. aeruginosa and K. pneumoniae* (Rao and others 2015). In another study by Morsy and others (2014), silver and zinc oxide (100 nm) nanoparticles were added to pullulan films and evaluated for their antbacterial activity against *L. monocytogenes, S. aureus, E. coli* O157:H7 and *S.* Typhimurium. The study showed that zinc oxide (100 nm) was the most inhibitory against all bacteria in the study.

Polymer-based films incorporated with other natural substances can be used to control pathogenic species on surface of food. Vargas and others (2011) used films made from a combination of high molecular weight chitosan and sun flower oil to assess their antibacterial action against mesosphilic bacteria and coliforms inoculated on pork meat hamburgers. The surface of both sides of hamburgers was coated with the chitosan films and held at 5^{o}C for 8 days. It was shown that there was reduction of 0.5-1 log mesophilic microorganisms and 1 log CFU/g for coliforms.

Another study by Siripatrawan and others (2012) used chitosan films incorporating 20% (w/v) of green tea extract to evaluate their antimicrobial activity

against mesophilic bacteria, yeasts and molds, and lactic acid bacteria (LAB) that could possibly contaminate the pork sausages held at 4^{o}C for 20 days. The experimentation results revealed that faster growth in control samples for total viable count and molds and yeast was observed but no difference for LAB was found.

Currently, a few studies have been conducted to evaluate the antibacterial properties of EO-added polymeric films against microbes on food surfaces. During food refrigeration, microbes mainly contaminate food on the surface. Thus, food packaging materials incorporated with EOs may represent an effective way to control microbial contamination of refrigerated foods. Morsy and others (2014) used pullulan films incorporated with oregano EO to control *E. coli* O157:H7 and *S.* Typhimurium on raw beef and *S. aureus, L. monocytogenes* as associated with ready-to-eat meats. The results showed that pullulan films incorporated with oregano EO reduced the cell numbers of *E. coli* O157:H7, *S. aureus* and *L. monocytogenes* by 3 log units but only reducing by 1 log the cell numbers of *S.* Typhimurium.

2.4.2 Mechanism of antimicrobial action of essential oils

Thyme, oregano and clove EOs contain bioactive phenolic groups such, as thymol, carvacrol and eugenol (Xu and others 2005). The antibacterial activity of these phenolic groups is thought to be due to the hydroxyl groups projected at different positions of their aromatic ring (Figure 2.1). Ultee and others (2002) found that the hydroxyl group of carvacrol caused membrane expansion and exhibited antimicrobial activity against *Bacillus cereus*. As components of EOs, phenols are fat-soluble and able to interact with the fatty acids in the bacterial cell membrane to cause a loss of cell membrane integrity.

The mechanism of the antibacterial activity of phenols depends on the type of EOs and the specific microorganism. It is commonly believed that Gram-negative bacteria are more resistant to hydrophobic antibiotics and toxic drugs than Gram-positive species. The reason is that Gram-negative bacteria have a highly rigid outermost membrane which consists of a lipopolysaccharide (LPS) molecule comprising of saturated fatty acid chains (Nazzaro and others 2013). It is the LPS that makes this outer membrane of Gram-negative bacteria serve as a penetration barrier toward higher molecular weight and hydrophobic compounds (Bolla and others 2011). However, certain EOs exhibit a phenolic property that causes modification of the fatty acid composition in the LPS membrane. For instance, Gram-negative cells treated with thymol, carvacrol and eugenol may have an increased amount of saturated C_{16} fatty acids and reduced amount of unsaturated C_{18} fatty acids in their outer membrane (Diplasqua and others 2006). Furthermore, phenols may affect a desaturase enzyme required for the biosynthesis of the outer membrane fatty acids (Nazzaro and others 2012). As a result, these changes disturb and disintegrate the LPS membrane of Gram-negative bacteria, thus making these species susceptible to the phenolic EOs.

Outer membrane proteins of Gram-negative bacteria may also play a significant role in channeling biological active compounds of EOs to the cell membrane. Due to the hydroxyl groups of phenols, membrane fluidity changes which in turn increases membrane permeability to the phenols (Nazzaro and others 2012). Holley and Patel (2005) found that thymol and carvacrol diffused across the cellular membranes of *E. coli* and *Salmonella* Typhimurium. This observation was attributed to the outer membrane porin proteins of Gram-negative species whose function is to channel macro nutrients to

the cell membrane and prevent toxins and antibiotics from getting inside the cell. In addition, porin proteins aid in the transport of phenols and hydrophilic compounds which eventually reach-targeted sites of the microbial cell.

The selective permeability of the cell membrane of Gram-negative and Gram-positive bacteria may be lost due to phenols. The hydroxyl groups of carvacrol and thymol are located on the aromatic ring structures of these compounds. The antimicrobial activity of carvacrol and thymol as phenolic groups of thyme, clove and oregano EOs is attributed to the presence of these hydroxyl groups. In the cell cytoplasm, carvarol liberates its protons and captures a cation (K+) when diffusing out of the cell membrane. As a consequence, cell death occurs following a disrupted metabolism. In addition, carvacrol disrupts the cell membrane by increasing its fluidity which in turn leads to increased cell permeability. As a result, cellular stress takes place following the release of the cellular contents, K^+ and ATP molecules outside of the cell (Holley and Patel 2005). Similarly, thymol disrupts cell membrane integrity by drastically altering the structure and functions of inner and outer membranes (Hyldgaard and others 2012). Thus, both phenolic compounds cause membrane damage which in turn induces the loss of K^+ followed by the leakage of cellular contents (Holley and Patel 2005).

Cinnamaldehyde and eugenol as present in cinnamon and clove, respectively, contain a benzene ring (Figure 2.1). The antibacterial activity of eugenol is similar to that of carvacrol and thymol. Once incorporated in the cell membrane, eugenol disrupts the surface and structural proteins. In addition, these phenolic groups in the EOs inhibit cellular metabolism and ATPase whereas cinnamaldehyde predominantly disrupts the bacterial cell membrane (Hyldgaard 2012). Other principles underlying the potential

antimicrobial action of phenolic compounds of EOs may be inhibition of energy production, disrupted process of ATP production or depletion of cellular energy and at high concentrations, protein denaturation occurs (Tiwari and others 2009).

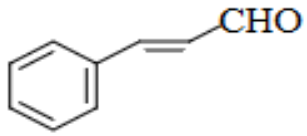

Cinnamaldehyde in cinnamon

Phenols in thyme, oregano and clove EOs

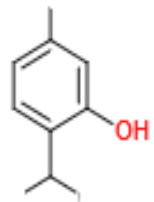

Thymol

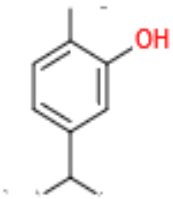

Carvacrol

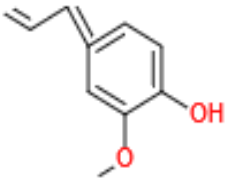

Eugenol

Figure 2. 1 Chemical structures of phenols and cinnamaldehyde

CHAPTER 3

MATERIALS AND METHODS

3.1 Chemical synthesis of antimicrobial nanocellulose-based films

Three biopolymers (nanofibril cellulose; NFC), chitosan, and poly (vinyl) alcohol (PVA) were used to prepare composite films via solution-blending and casting techniques. First, 5% (w/v) PVA (99-100% hydrolyzed, approx. MW 86,000, Acros Organics, Morris Plains, NJ, USA) were fully dissolved in distilled water by heating in the autoclave at 121^{o}C for 30 min.

Simultaneously, 1% (w/v) chitosan (MW 190000-310000 Da, Sigma Aldrich, St. Louis, MO USA) and 2.3% (w/v) NFC (90% fines, University of Maine, Orono, ME, USA) solutions were separately prepared by dissolving (at room temperature and moderate stirring at 3.4×g) low molecular chitosan and NFC in 1% acetic acid solution (Schnuck's Markets, Inc., St. Louis, MO, USA) and distilled water respectively. Then, 4.0 g glycerol (Sigma Ultra, approx. 90% GC) and 0.4 g of Tween 80 (Polysorbate), Sigma Aldrich, St. Louis, MO, USA) were incorporated into the NFC dispersion and the mixture was kept stirred at the above-specified conditions. Then, the PVA and chitosan solutions were mixed together and stirred at 3.4 ×g and 90^{o} for 1 h, after which NFC-glycerol suspension was added to the PVA-chitosan composite solution. The film blend was obtained by homogenizing the polymer solution mixture at 90^{o}C and 350 rpm stirring for 2 h followed by 15 min of sterilization in the autoclave at 121^{o}C and 15 psi.

Thereafter, 5% (v/v) of 10% pure essential oil solutions that were prepared by diluting pure cinnamon (Now Foods, Bloomingdale, IL, USA) and clove (Now Foods) with dimethyl sulfoxide **(**Sigma Aldrich) were gradually added to the sterile

homogeneous polymeric film solution and the blend was stirred again at 90^{o}C and 3.4 ×*g* for 1 h.

For antimicrobial supplemented films, three individual batches of the NFC–PVA-based composite films in accordance with the treatments were made as shown in Table 3.1 below.Finally, 15 mL of the sterilized blend for film-forming solution were used to cast the films on the 12cm ×12 cm sterile plastic plates (Greiner, Bio-One, Mosonmagyaróvár, Hungary) and air dried in the laminar air hood (Environmental Systems, Westinghouse, Grand Rapids, MI, USA) at 25^{o}C for 13- 15 h. After drying, the film-containing plates were covered, wrapped with aluminum foil, and stored at 4^{o}C for physical characterization and antimicrobial studies.

Table 3. 1 Incorporation of antimicrobials into NFC-PVA films

Treatment	**PVA (% w/v)**	**Glycerol (% w/v)**	**NFC (% w/v)**	**Chitosan (% w/v)**	**Clove (% v/v)**	**Cinnamon (% v/v)**
T0 (negative control)	----	-----	----	-----	-----	-----
T1 (control)	5	4	2.3	1	-----	-----
T2	5	4	2.3	1	-----	0.5
T3	5	4	2.3	----	0.5	------

3.2 Antimicrobial film - agar assays

Essential oils (EOs) of clove and cinnamon were tested for their antibacterial activity against four important groups of food pathogenic strains using a film-agar assay technique. The strains of Shiga toxin producing *Escherichia coli* (STEC) O157:H7

(505B, EDL-933, C7927, 3178-85, and MF-1847), *Staphylococcus aureus* (DLV1, FRI, 183B, and β-hemolytic), *Listeria monocytogenes* (7644, V373E, Murray, Scott A and Brie) and *Salmonella* strains (*S.* Enteritidis I4-9, *S.* Enteritidis I4-10, *S.* Typhimurium 789 and *S.* Typhimurium 14028) were from the Food Microbiology Laboratory of the University of Missouri, Columbia and used in this study.

Twenty-four hour-grown inocula (approximately 10^9 CFU /mL) of *E. coli* O157:H7 and *S. aureus* strains were freshly prepared by growing cells in enriched Tryptic soy broth (Becton, Dickinson and Company, Sparks, MD, USA) at 37°C while that of *L. monocytogenes* strains was prepared by growing cells in Brain Heart Infusion (BHI) broth (Merck Millipore, Billerica, MA, USA) in an aerobic shaker incubator set at 37°C and 160 rpm shaking.

A 0.25 mL volume of freshly grown (24 h) bacterial suspension was evenly seeded onto the entire surface of Mueller Hinton agar plates for *E. coli* O157:H7 and Heart Brain Infusion agar plates for *S. aureus*, *Salmonella* spp. and *L. monocytogenes* using sterile glass spreader. Utilizing a sterile scalpel or razor blade, uniform 2 cm × 2 cm squares were aseptically cut from the control (PVA/NFC) films and those prepared with antimicrobials. Then each cut film square was placed 4cm apart on the surface of the inoculated agar using a sterile pair of forceps. The plates were incubated aerobically at 37°C for 24 h. The antibacterial activity was assayed by visualizing inhibition zone or turbidity (cloudiness) of the film cuts after 24 h.

3.3 Preparation of the strain cocktails

Fresh overnight cultures (10^9 CFU/mL) of *E.coli* O157:H7 strains (505B, EDL-933, C7927, 3178-85, and MF-1847) were individually grown in the Tryptic Soy Broth (TSB) and incubated in an aerobic shaker incubator set at 37°C and 160 rpm shaking for 22 h.

One liter of the STEC O157:H7 strain cocktail (1.8×10^{10} CFU/mL) was prepared using overnight grown strain cultures (10^9 CFU/mL) of *E. coli* O157:H7 at a ratio of 1:1 of each strain. One liter of the mixed strain cocktail was dispensed into sterile centrifuge tubes then aliquots of 10 mL strain cocktail were subject to high speed centrifugation (491.1 ×*g* at 25°C) for 10 min. After that, the supernatant was discarded and cells pellets were diluted with 10 ml peptone water.

The peptone-diluted cultures were rewashed by centrifuging them at 491.1 ×*g* for 5 min and dumping the supernatant out. Then the TSB-free cell pellets were ice-chilled in the refrigerator at 4°C for 24 h. Afterwards, 5 mL of diluent (peptone water) were added to the cell pellets to form a concentrated cocktail cell suspension of approximately 2×10^{10} CFU/mL. Finally, the optical density (OD) at 600 nm was checked and ten-fold dilutions of the strain cocktails were performed to determine the viable cell counts on Plate Count Agar (PCA).

3.4 Food model studies

Four film treatments in duplicates (T1=no film, T2=NFC-PVA-chitosan, T3=PVA-NFC-chitosan + 0.50% clove and T4=PVA-NFC-chitosan-0.50% cinnamon) for each of two separate replications (Figure 3.1) were made in order to investigate the antimicrobial activities of these polymeric films against growth of *E. coli* O157:H7 strains on raw beef.

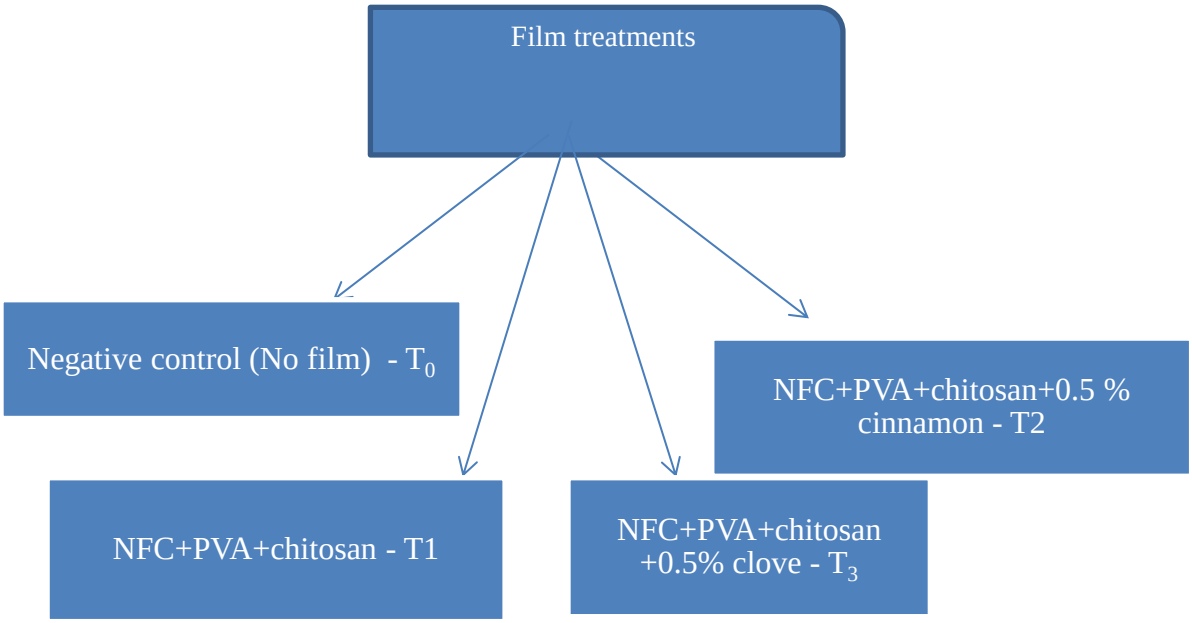

Figure 3. 1 Film treatments for beef with *E. coli* O157:H7 inocula

Beef top round roast (purchased from Lucky Market, Columbia, MO, USA) was initially frozen and later held at 4^{o}C overnight prior to inoculation with STEC O157:H7. Then, beef top round roast meat was aseptically cut into (2.5 cm × 2.5 cm × 1.25 cm) pieces using sterilized meat corers and sharp knives on a sanitized cutting board in a laminar air flow hood. Finally, meat pieces were conditioned on ice and refrigerated overnight prior to inoculation and wrapping with the antimicrobial films

For beef inoculation with STEC O157:H7 inoculum, one piece of beef (27.5 cm^2) was submerged in 15 mL of a cocktail's inoculum (1.7×10^{10} CFU/mL) prepared from *E. coli* O157:H7 strains for 2.5 min. After that, each inoculated piece was aseptically pierced using a sterilized paper clip and hung 30cm above an aluminum foil covered-tray and allowed to drip-dry in the laminar airflow hood for 15 min (Figure 3.2).

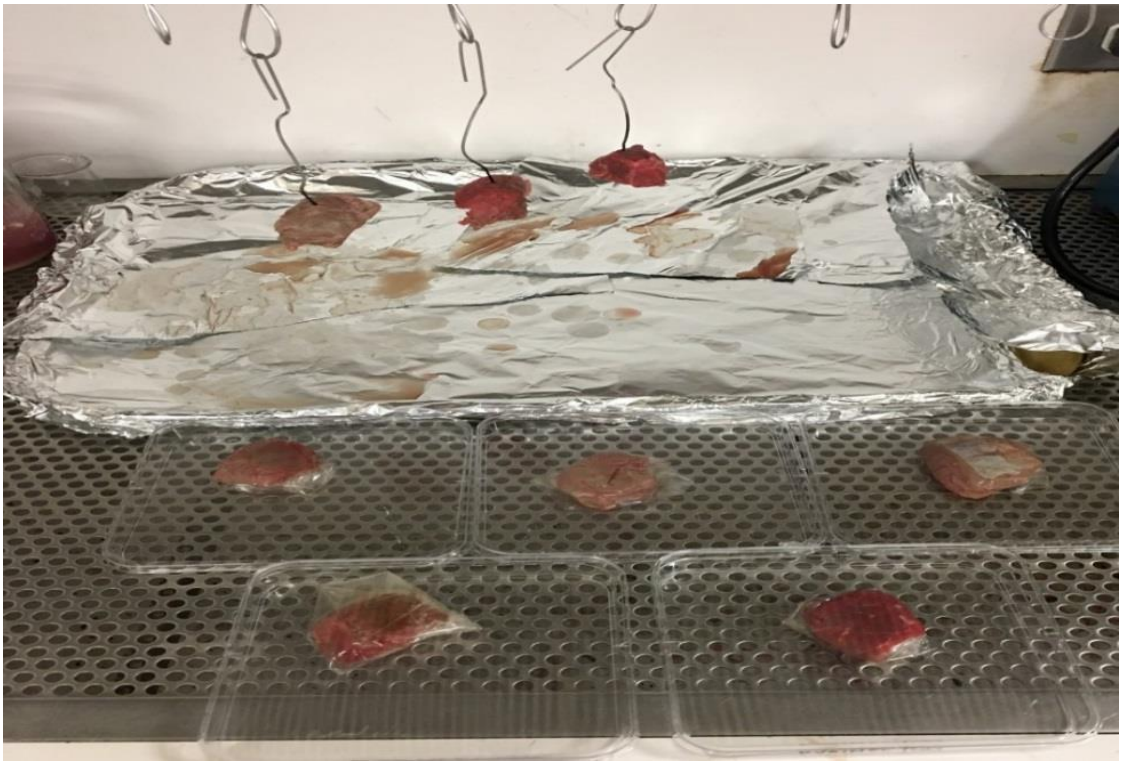

Figure 3. 2 Drip-drying of beef pieces with *E. coli* O157:H7 inocula

After meat inoculation, each of the meat pieces for controls and for day 0 treatments in duplicates was immediately transferred and weighed in a sterile stomacher bag, diluted (1:10) with buffered peptone water and stomached for 2 min. The day 0 meat broths were then serially diluted and 0.1 mL from 10^{-4} up to 10^{-6} dilutions were individually seeded onto MacConkey sorbitol agar medium to obtain initial counts for *E. coli* O157:H7 in raw beef. To investigate the presence of *E. coli* O157:H7 and total background flora counts in the beef, two un-inoculated beef pieces were also diluted (1:10) with buffered peptone water and homogenized for 2 min.

The resulting broth was then serially diluted with peptone water to obtain dilutions of 10^{-2} up to 10^{-5}. Then, 0.1 mL of each of the diluted meat broths was transferred and spread onto MacConkey sorbitol agar medium for detecting the presence

of initial *E. coli* O157:H7 colonies in the beef and 1 mL of it was pour-plated using PCA for enumerating the beef initial total counts. The colony counts (CFU/cm^2) were determined after 24 h of aerobic plate incubation at 37ºC.

Finally, the antimicrobial activity potential of the synthesized polymeric films was assayed by wrapping *E. coli* O157:H7-inoculated beef in the films and conducting plate counts.

Beef-antimicrobial film treatments in duplicates of the same film synthesis batch (T1=Chitosan –PVA NFC films, T2=Chitosan-PVA-NFC+0.50% cinnamon films and T3= Chitosan-PVA-NFC+0.50% clove films) and those marked as absolute negative controls (T1=no films) were respectively held at 4ºC for up to 10 days.

Sampling and plate counting were periodically conducted at 3, 6 and 10 days of beef cold storage. Beef pieces in duplicates were serially diluted (1:10) and homogenized for 2 min, then 0.1 mL of the diluted meat broths was seeded onto MacConkey sorbitol agar medium and colorless STEC O157:H7 colonies were counted following 24 h of aerobic plate incubation at 37ºC. Beef treatments and plating were arranged in duplicates in each of the two experimental duplications.

3.5 Beef shelf-life studies

Beef round top roast meat pieces (2.5 cm × 2.5 cm × 1.5 cm) were each wrapped in the synthesized antimicrobial films following film treatments shown in Figure 3.1. First of all, the meat pieces for day 0 and absolute negative control treatments were individually diluted (1:10) with buffered peptone water and stomached for 2 min. Total colony counts on PCA medium were determined after 24 h of plate incubation at 37ºC.

For beef-film treatments, each meat piece in duplicates was wrapped in the antimicrobial film and total plate counts were periodically determined at 3, 6 and 10 days

of cold storage at 4^{o}C. The meat piece was diluted (1:10) with buffered peptone water and homogenized for 2 min. The meat broth was then serially diluted up to 10^7 and 1 mL of it was pour-plated using PCA medium and plates were incubated at 37^{o}C for 24 h. Finally, the total counts were determined and expressed as CFU/cm^2. The experiments were performed in duplicates and two replications.

3.6 Physical characterization of PVA-NFC-chitosan composite films

3.6.1 Tensile stress and elongation at break measurements

First, the NFC-PVA-chitosan composite films and those incorporating EOs were cut into rectangular-shaped strips with dimensions of 20 mm width and 62.5 mm length and peeled off the plates. The thickness of the film strips was measured using a caliper (sensitivity of ± 0.01 mm) before proceeding to tensile strength and elongation at break measurement tests. The thickness was randomly measured along each of the four sides of film specimens and the mean value (mm) of the thickness was calculated.

As described in the ASTM method D882-02 (ASTM 2002), tensile strength (TS) and elongation at break (% EB) or fracture strain (FS) as well as elastic modulus of the prepared NFC/PVA composite films were measured using a texture analyzer (Texture Technologies Corp., Scarsdale, NY, USA) with the aid of a 5 kg load cell at 25^{o}C.

Initially, the grip separation, distance and cross-head speed were set at 50mm, 40mm and 5 mm/min respectively. Prior to analyzing the film specimens, the TA probe (TA version N^{o} 07.144) was calibrated using a return distance of 25 mm with a contact force of 30 g. Thereafter, the pre-cut rectangular film strip was mounted into the grips and pulled apart. A force (N) versus time (s) and distance (mm) graph was constructed by a texture analyzer program software as the specimen is pulled apart and allowed to return to its initial position. The TS (Pa) was calculated by dividing the maximum force (N) by

the initial cross-sectional area (thickness x width, m^2) of the specimen. EB (%) was determined by multiplying the ratio of the changed length (Δx, mm) at the point of sample failure to the initial length (X_0, 62.5 mm) of a specimen by 100. From data obtained with this method, the elastic (Young) modulus (Pa) was determined as the quotient of the tensile stress and the elongation at break of the film specimen. The physical measurements were carried out in duplicates and in two replications.

3.6.2 Characterization of the polymeric films with Fourier Transform Infrared (FTIR) Spectroscopy

The presence of specific chemical groups in the synthesized polymeric films was characterized using Fourier transform infrared (FTIR) spectroscopy. PVA/NFC films with respect to their treatments were cut into square-shaped specimens (0.25 cm^2) and placed over the diamond. The specimen analysis was carried out to obtain infrared spectra of diamond in the range of 3500-800 cm^{-1} during 64 scans with 2 resolutions $.cm^{-1}$. For each film treatment, three specimens were analyzed in duplicates and analysis was carried out in two replications with this characterization technique.

After that, individual film components such as aqueous PVA, NFC, glycerol and chitosan as well as essential oils and distilled water were analyzed with FTIR to obtain their corresponding absorption spectra. In addition, films prepared from only one polymer ingredient without addition of glycerol were also analyzed with FTIR. The individual peaks indicating specific chemical groups for each ingredient spectra were the compared on case by case basis to those present in the spectra of films from each treatment. The similarity in shapes and regions of sample absorption spectra were then used to identify specific chemical groups in the analyzed polymeric films and relate them to the detectable ingredients in the films.

3.6.3 Characterization of the film surface with scanning electron microscopy and Energy dispersive X-ray spectroscopy

The surface morphology of the film specimens was examined using scanning electron microscopy (SEM). First, the films (prepared by drying in the oven at 45^{o}C for 30 h) were cut into rectangular shapes. The film specimens were then mounted on stubs (containing electrically-conductive tape) for the scanning electron microscope. The SEM images were then obtained using a low beam (<70%) with magnification power (2500-5000×).

The surface elemental composition and mapping of the same film specimen mounted on stubs was also examined using Energy dispersive X-ray spectroscopy (EDS). At least seven spots for rough and smooth surface of each film specimen in duplicates and two replications were analyzed to identify and quantify (relative atomic percentage) chemical elements as located in the micrographs of the polymeric films. A Quanta Espirit Bruker Microanalysis software was used to process data obtained with EDS test.

3.6.4 Color of the films

The color of the film specimens was measured using a color meter which was placed over a film specimen and light reflected over it. The color meter readings were values for rectangular coordinates (L*, a* and b*), where L*(0-100) indicate black to white, a* values indicate color range from red to green and b* values indicate yellow to blue. The color readings were used to compare the L*, a* and b* coordinates of each film containing essential oils to those containing chitosan as the control group. The color difference (ΔE) of the film samples was then computed using this equation: $\Delta E=[(\Delta L^*)^2 + (\Delta a^*)^2 + (\Delta b^*)^2]^{0.5}$

3.7 Statistical analysis of data

To evaluate antimicrobial activity, mechanical and sensory properties of the synthesized films, data for films treatments (wrapped beef: T1, T2 and T3) used in the food model studies as well as those used for mechanical property and color assessment were statistically analyzed and compared to those of the controls (T0: unwrapped beef) and among themselves. In this regard, ANOVA and Turkey's least significance difference (LCD) tests were used following the SAS GLM procedure (Copyright © 2008, SAS Institute Inc., Cary, NC, USA) to determine if there are significant differences among film treatments and controls with a level of significance ($\alpha = 0.05$). The comparisons among treatments and controls were performed considering means sharing the same letter (A, B or C) to be not significantly different and those not sharing letter to be significantly different.

CHAPTER 4

RESULTS AND DISCUSSION

4.1 Microbial studies

4.1.1 Film-agar assays

Initially, a number of essential oils (EOs) were screened for their inhibitory activity against growth of 18 pathogenic strains of Shiga toxin producing *Escherichia coli* (STEC) O157:H7, *Salmonella* spp., *Staphylococcus aureus* and *Listeria monocytogenes* using agar diffusion method. The screening data showed that cinnamon and clove at lower concentrations of 0.25-0.5% exhibited good bacteriostatic effects on the bacterial strains tested (data not shown). In the films with 1% chitosan, 0.50% clove and 0.50% cinnamon were assayed for their potential antibacterial activity against growth of the strains in the afore-mentioned bacterial groups using the film-agar assay technique. With this method, the experimental findings showed that PVA-CNF films incorporated with 1% chitosan had antimicrobial effect on some of the tested strains to a lesser extent.

Antibacterial activity of chitosan may be explained by the fact that there might be some residual acidity on the film surface due to chitosan solution prepared using 1% acetic acid (Zvanovic and others 2005). Another reason for chitosan antimicrobial activity is that some of the positively charged NH_2 groups from chitosan solubilization in aqueous acid (1% acetic acid or 1% lactic acid) could have stayed on the film surface and once in reaction with negatively charged groups on the surface of the bacterial cell membrane, cell disruption and death occur. Furthermore, antimicrobial activity of chitosan films can be a result of diffusion of positively charged chitosan molecules into the agar medium, thus creating zones of inhibition (Wang and others 2011).

Films containing chitosan and EOs exhibited antimicrobial properties to a greater extent of inhibition against most of the potentially disease-causing bacterial strains used in this study. Table 4.1 shows the degree of inhibition of the antimicrobial PVA-cellulose based films prepared using 1% chitosan, 0.50% clove and 0.50% cinnamon. Data indicate that all strains of STEC O157: H7, two strains of *Salmonella* Enteritidis (I4-9, I4-10) and *Salmonella* Typhimurium 789, two strains of *L. monocytogenes (*Murray and Brie*)* were strongly inhibited by 0.50% cinnamon and 0.50% clove in the PVA-NFC films. In this study, the effect of EO-chitosan combination in the films on the growth of the same food pathogens was also investigated. It was deduced that the synergistic bacterial inhibition effect due to chitosan- EOs on *E. coli* O157:H7 and *Salmonella* spp. strains is greater than compared to other strains in the study.

The films incorporating 0.10- 0.75% EOs were used to test for their inhibitory activity against the being-studied pathogenic strains mentioned-above. The study revealed that there were no differences to use EOs concentrations that are higher than 0.50%. Moreover, it was observed that EOs were on the film surface and could not diffuse to the surroundings during film drying or storage period. This fact was also observed during the agar-film assays where no zones of inhibition were formed around film strips that were placed on the agar medium. This could be due to the EOs – polymeric matrix interaction, which often limits diffusion of EOs out of the film system, thus achieving high antimicrobial activity of the films (Wang and others 2011).

The mechanism of inhibitory activity of essential oil-components on bacteria has been elucidated in a number of studies (Morsy and others 2014; Nunez and D'Aquino 2012; Sharma and others 2014). Several low molecular components of EOs, such as

terpenes and terpenoids, thymol, eugenol and carvacrol, cinnamaldehyde and aromatic components have been reported to act as antibacterial agents in EOs (Quazzou and others 2011). Cinnamaldehyde in cinnamon and phenols interact with the bacterial cell membrane often resulting in the cell dysfunction and loss of specific cell permeability (Wang and others 2014). Moreover, carvacrol makes energy unavailable to the cell functions and the cell membrane highly permeable to proteins and K^+.

Table 4. 1 Degree of inhibition of PVA-NFC based films with incorporated clove, cinnamon and chitosan against growth of selected pathogenic strains

Bacterial strain	**PVA/NFC films with 0.5% clove**	**PVA/NFC films with 0.5% cinnamon**	**PVA/ NFC chitosan films**	**PVA/NFC films**
E. coli O157:H7 C7927	++++	++++	++	-
E. coli O157:H7 EDL-933	++++	++++	++	-
E. coli O157:H7 MF-1847	++++	++++	++	-
E. coli O157:H7 505B	++++	+++	++	-
E. coli O157:H7 3178-85	+++	+++	+++	-
L. monocytogenes Murray	++++	++++	++	-
L. monocytogenes Brie	++++	++++	-	-
L. monocytogenes Scott A	++	+++	-	-
L. monocytogenes V373E	++	++++	-	-
L. monocytogenes 7644	+++	++++	-	-
S. aureus β-hemolytic	-	++++	-	-

S. aureus DLV1	+++	+++	-	-
S. aureus FRI	+++	+++	+	-
S. aureus 183B	++	+++	-	-
S. Enteritidis I4-9	++++	++++	++	-
S. Enteritidis I4-10	+++	++++	++	-
S. Typhimurium 789	++	+++	+	-
S. Typhimurium 14028	+	++	-	-

++++: very strong inhibition: **+++**: strong inhibition **++**: weak inhibition

+: very weak inhibition **-** : no inhibition

4.1.2 Preparation of the strain cocktails

Figure 4.1 shows the OD values versus the strain counts (CFU/mL) *E. coli* O157:H7 involved in this study. As seen from this figure, the OD_{600} values for *E. coli* O157:H7 strains as grown in the TSB at 37°C for 22 h appear close to each other. This gave rise to approximately equal counts of individual strains. The cocktail composed of these strains grown in the conical flasks and aerobic shaker at 37°C for 22 h was prepared for food model experiments. The cocktail counts were 4.1 and 6.1×10^9 CFU/mL of *E. coli* O157:H7 for the first and second replications, respectively.

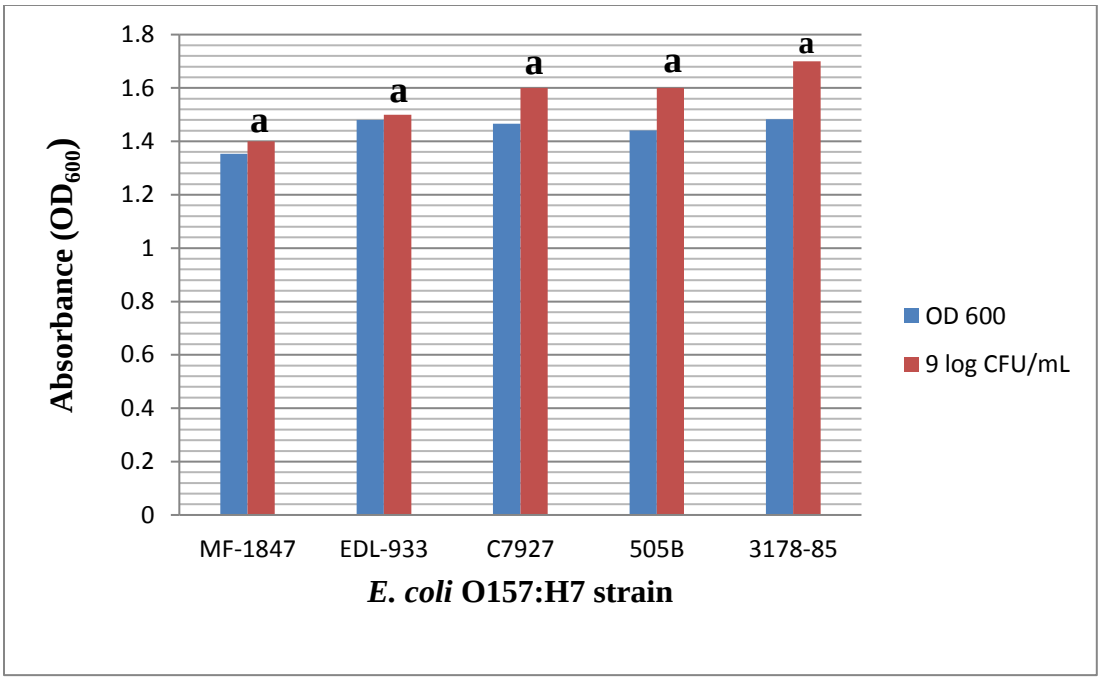

Figure 4. 1 Absorbance (OD_{600}) versus counts (10^9 CFU/mL) of *E. coli* O157:H7 strains grown at 37°C for 22 h

4.1.3 Food model studies

4.1.3.1 Effect of antimicrobial films on growth of E. coli O157:H7 on raw films

The effect of antimicrobial composite films synthesized from blending NFC-PVA chitosan with 0.50% EOs were used to investigate the effect they might have on growth of *E. coli* O157:H7 on raw beef. The figure 4.1 shows the comparison between combined effects of beef-*E. coli* O157:H7 treatments with NFC-PVA films containing 1% chitosan and those incorporating both 1% chitosan and 0.50% EOs (clove or cinnamon). Beef was artificially contaminated with *E. coli* O157:H7 and treatment samples were wrapped in the films containing either chitosan or chitosan-EOs and kept at 4°C for up to 10 days. Figure 4.1 presents the average counts of *E. coli* O157:H7 on raw beef as treated (T1, T2 and T3) and untreated (T0-controls) in duplications and two replications.

From this figure, it is apparent that the number of *E. coli* O157:H7 on treated beef (T1, T2 and T3) was significantly reduced ($P \leq 0.05$) as compared to controls. For instance, there were approximately two log reductions of *E. coli* O157:H7 cells on beef wrapped with chitosan and EOs-containing polymeric films. Conversely, there were two log unit increases in the population of this organism on untreated beef after 10 days of storage at 4^{o}C.

The collected data in this study were statistically analyzed using ANOVA and Tukey's least significance difference (LSD) test method to test the difference in growth inhibition of *E. coli* O157:H7 on beef samples. The test showed that there were significant differences ($P \leq 0.05$) between the treatments (T1, T2 and T3) and the controls (T0) and no significant difference ($P > 0.05$) among the treatments (T1, T2 and T3) at a 5% level of significance.

As seen in Figure 4.2, the effect of chitosan–containing films on growth reduction of *E. coli* O157:H7 on raw beef is obvious and can be elucidated either in the presence or absence of EOs in the films. This observation could be explained by the fact that the antibacterial activity of chitosan is effectively expressed when it is in aqueous state (Zivanoc and others 2005). On one hand, chitosan–containing films were becoming moist as they absorbed moisture from the juices of the beef cuts, hence becoming more effective at reducing growth of *E. coli* O157:H7 on raw beef.

On the other hand, EOs consist of hydrophobic component (Quazzou and others 2011) which when incorporated in chitosan-containing films, prevent beef moisture from reaching the charged chitosan groups in the composite system. Thus, inhibitory activities

exhibited by the films incorporated with EOs are possibly due to the cinnamon and clove EOs.

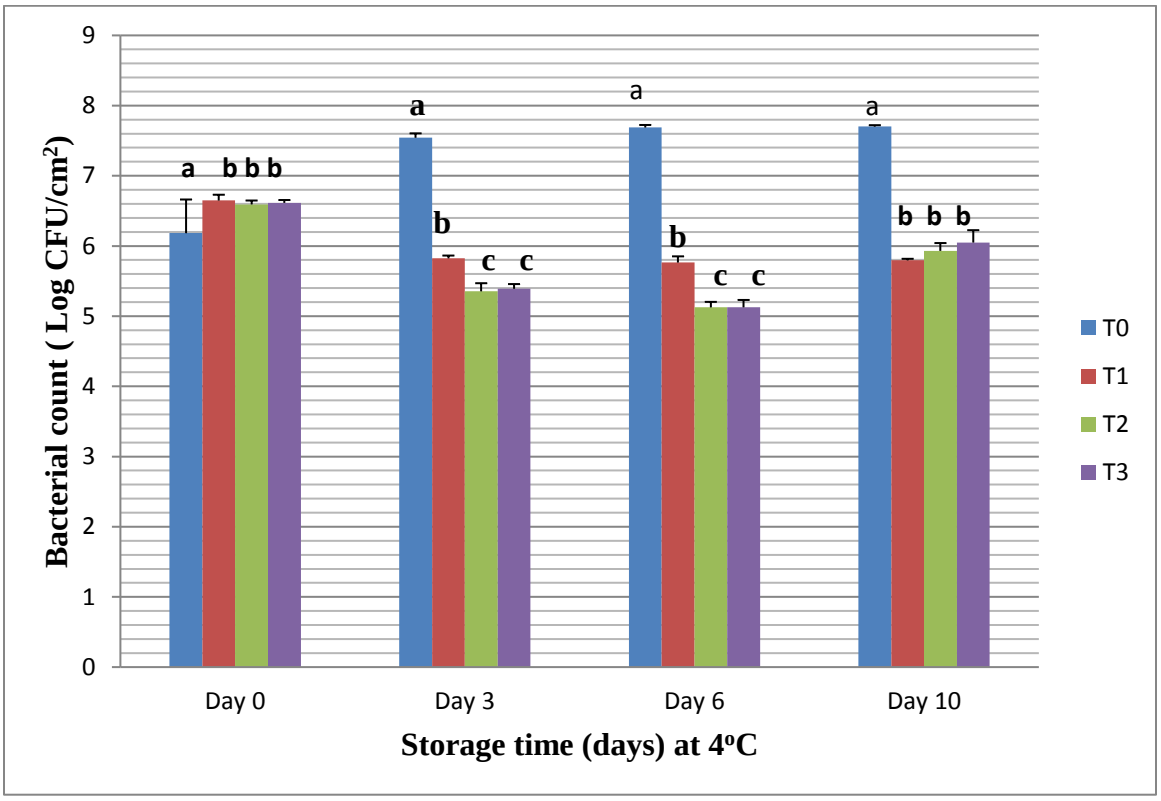

Figure 4. 2 Effect of chitosan, clove and cinnamon-incorporating films on growth of *E. coli* O157:H7 on raw beef

Thus, inhibitory activities exhibited by the films incorporated with EOs are possibly due to the cinnamon and clove EOs. The antibacterial activity of these EOs when added to the films is higher than when used in liquid state (Wang and others 2011). When incorporated in the polymeric films, the film matrix limits the diffusion of EOs out of the composite system. Thus, the inclusion of chitosan or chitosan -EOs in the film matrix resulted in films with the capacity of significantly inhibiting growth of *E. coli*

O157:H7 on raw beef even though lower storage temperatures may have impact on growth of this bacterium.

4.1.3.2 Shelf-life of raw beef wrapped in the NFC-PVA films

Figure 4.3 shows the growth curves of background flora and other bacteria in beef pieces wrapped with NFC-PVA composite films incorporating 1% chitosan and 0.50% EOs. Samples were held in a refrigerator at 4^{o}C to mimic the storage conditions under which raw beef is kept prior to consumption. Overall, after 10 days of cold storage, there were 3 log CFU increases in total counts for beef in either treatment as compared to their corresponding initial (day 0) counts.

Comparing treated beef to controls, approximately half-total count (3 logs) reduction in raw beef treated with either polymeric films containing chitosan or those containing both chitosan and EOs were achieved. The results shown in the figure 4.3 are the averaged counts (CFU/cm^2) obtained from samples with duplications and in two replications. The results obtained from these two replications were statistically tested at a 5% level of significance to show the statistical differences between the controls and treatments or treatments among themselves. The test results showed that the effects of film with 1% chitosan and those containing chitosan- EO combination on growth of *E. coli* O157:H7 on raw beef were not significantly different ($P > 0.05$) from each other but significantly different ($P \leq 0.05$) from the controls (untreated beef).

Figure 4.3 shows comparable growth trends of beef flora and spoilage bacteria in beef treatments and controls. As seen on this figure, the bacterial total counts in beef treatments (except T3) and controls were not significantly different in 6 days. Even though the total counts in treated beef sharply increased between day 6 and day 10, there

was growth inhibition due to films to some extent (Figure 4.3), since approximately half of the total count of bacteria in beef was reduced as compared to the controls

This implies that the total count reduction of bacteria in beef has only taken place on the beef surface which is ultimately in contact with the wrapping films. Thus, it follows that the shelf-life of beef treated under the same conditions could be limited to 6 days.

\

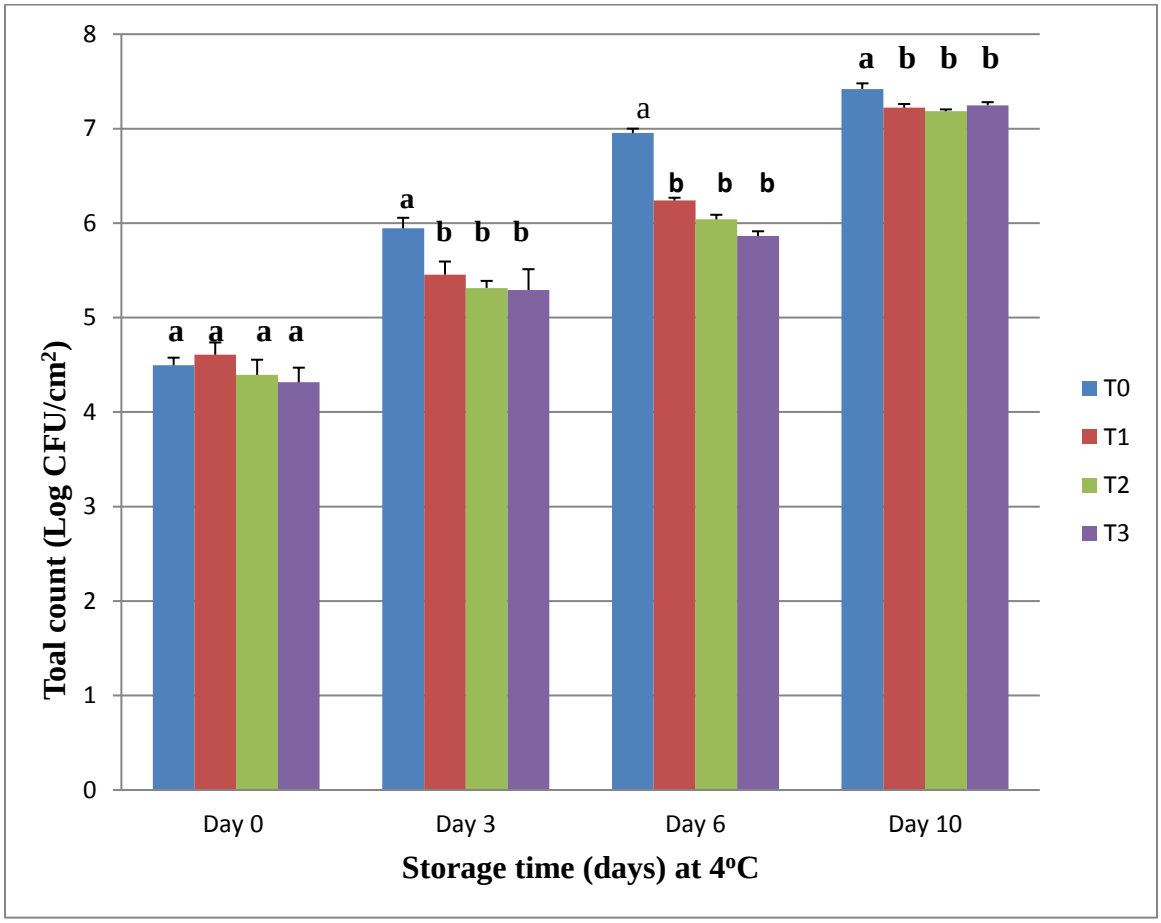

Figure 4. 3 Effect of antimicrobial films on total counts (CFU/cm^2) of raw beef (T0- no film T1: film with chitosan T2: film with chitosan +0.5% cinnamon T3: film with chitosan + 0.50% clove)

Taking differences in inhibitory activity of two kinds of EOs into account, it is clear that cinnamon EO-added films demonstrated stronger inhibitory activities than

clove-incorporated films (Figure 4.3) even though their effect on total count reduction was not significant ($P > 0.05$). This observation is in agreement with those of other studies (Lopez and others 2007; Valero and Salmeron 2003) that found that cinnamon has stronger antimicrobial activity than clove when used in liquid state. Another study by Wang and others (2014) revealed that cinnamon had strongest inhibitory activity against growth of *E. coli*, *S. aureus*, *Aspergillus oryzae*, and *Penicillium digitatum*.

4.2 Physical characterization of the films

4.2.1 Tensile properties

Figures 4.4 and 4.5 demonstrate the averaged values for tensile stress (TS, MPa, modulus of elasticty (ME, MPa) and tensile strain or elongation at break (%EB) of the polymeric films in each treatment (T1 = PVA-NFC films with chitosan, T2 = PVA-NFC films with chitosan + 0.50% clove, and T3 = PVA-NFC films with chitosan+ 0.50% cinnamon). As indicated in Figure 4.4, the changes in the TS, % EB as well as ME between control films (PVA-NFC films with chitosan) and those containing 0.50% EOs are obvious. For instance, the films incorporating chitosan had much higher TS and % EB values than those incorporating EOs. As seen in Figures 4.4 and 4.5, PVA-NFC chitosan films had TS and % EB of 2.89×10^7 Pa and 75.58%, respectively. Incorporation of 0.50% clove and 0.50% cinnamon EO into PVA-NFC chitosan films affected their tensile properties (Figure 4.4).

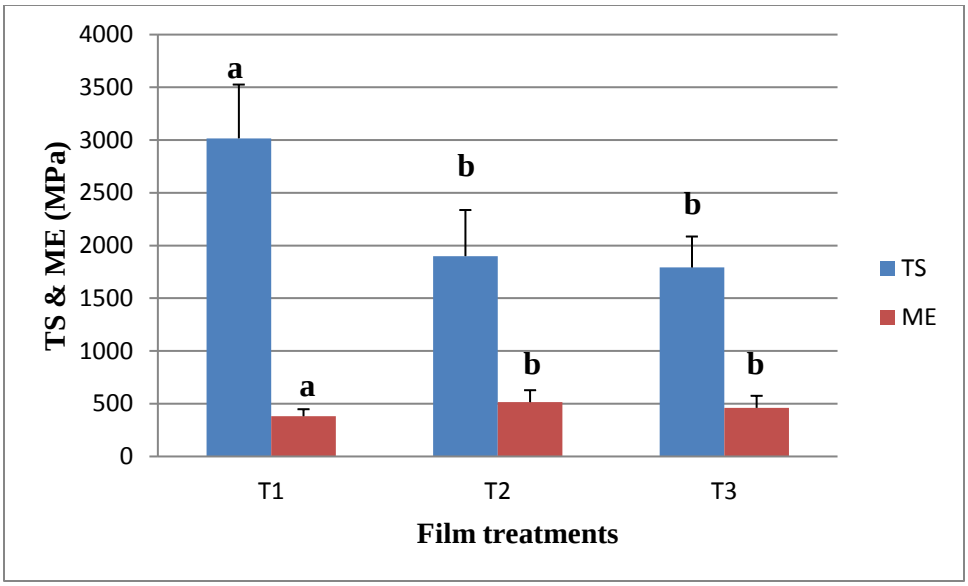

Figure 4. 4 Tensile properties of the PVA-NFC chitosan films and those incorporated with 0.5% EOs

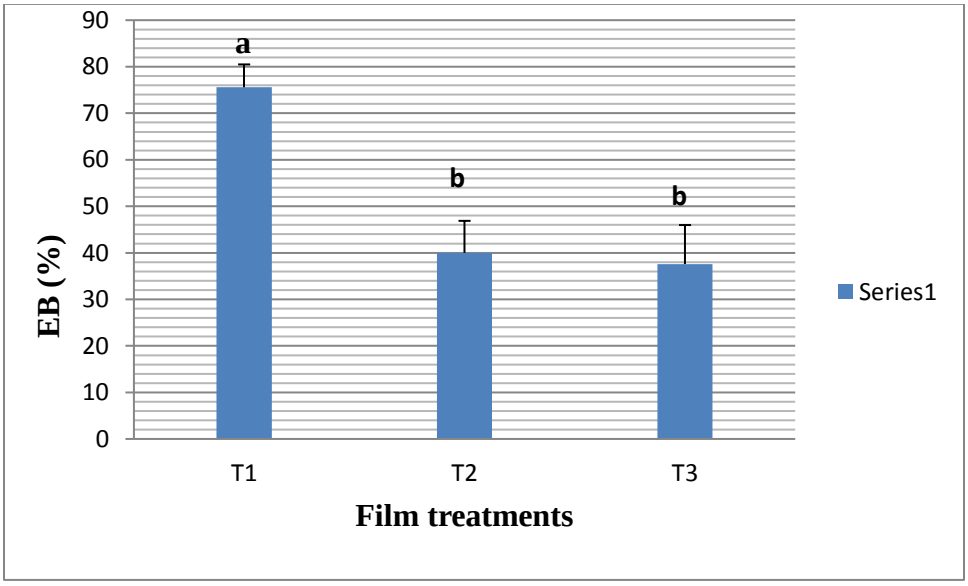

Figure 4. 5 Tensile strain (%) of the PVA-NFC chitosan films and those incorporated with 0.5% EOs

The TS and EB of these polymeric films were decreased by 38.0% and 47.0 % respectively in clove-incorporating films whereas these tensile properties in films with

cinnamon were reduced by 34.3% and 50.24%. However, the antagonistic effect of EO inclusion in the chitosan-containing films on modulus of elasticity (ME) was observed. The results in Figure 4.4 show that EOs-incorporated films had higher ME values compared to PVA-NFC chitosan films.

A comparison of the tensile properties for polymeric films as depicted in Figures 4.4 and 4.5 was made between the three treatments. Overall, TS, % EB and ME of the chitosan–containing PVA-NFC films were significantly different from PVA-NFC chitosan films incorporating EOs

($P \leq 0.05$). However, the tensile data for films with cinnamon and those for clove added-films showed that they were not significantly different ($P > 0.05$). Therefore, these results suggest that PVA-NFC chitosan films are more flexible and elastic than those incorporating EOs.

The difference in tensile properties can be related to a number of intrinsic factors in the polymer-based films. On one hand, tensile properties of the films are improved through the network microstructure and interactions in the polymer matrix due to an extending number of hydrogen bonds from chitosan and NFC the polymeric films (Sundaram and others 2016). On the other hand, incorporation of EOs into the polymeric films substantially lowered their flexibility and extensibility much more than the control chitosan films. The results in Figures 4.4 and 4.5 show that high TS and EB values are seen in the films containing clove as compared to cinnamon-incorporated films.

The decline in TS and EB of EOs-added films can be explained by the cross-linking effect due to EOs-polymer interaction. In fact, functional groups in the polymers, such as chitosan, may strongly interact with EOs to form covalent bonds, often leading to limited polymer-polymer interactions through hydrogen bonding. The interactions of polymers

with EOs in the films prevent the EO migration as the EO components are trapped within the films due to polymer-EO interaction. Increase in the EO concentration results in a greater molecular contact between functional groups and weaker intermolecular forces. This in turn, results in films with a smaller degree of stretchability and lower resistance to break (Cano and others 2015).

Phenols from EOs can form hydrogen and covalent bonds with functional groups of chitosan matrix (Hu and others 2009) or simply hydrogen bonds with hydroxyl groups of nanocellulose, poly (vinyl) alcohol (PVA) and a plasticizer. Jiarpinijnum and others (2013) investigated the interaction of EOs with chitosan in the films using Fourier transform infrared (FTIR) spectroscopy. The band at 1649 cm^{-1} led them to confirm that an amine group of chitosan and carbonyl group of cinnamon EOs were interacting. Additionally, an imine absorption band at 1600 cm^{-1}, formed as a result of chitosan-EO interaction, revealed the formation of a Schiff base. In another study by Azevero and Kumar (2012), cinnamaldehyde was shown to react with a chitosan functional group to form a Schiff base which subsequently induced a cross linking of the chitosan polymer. Other studies on cinnamon EO-added chitosan films also reported that cinnamaldehyde can act as a cross linking agent with chitosan (Ojah and others 2010; Higueras and others 2015; Lopez-Mata and others 2015). While interacting with functional groups of polymers in the films, EOs cause pronounced changes in the mechanical properties that are usually related to the film microstructure and intermolecular forces (Ataré and others 2010).

Other significant factors influencing tensile properties of the polymeric films are plasticizers, such as glycerol (Liu and others 2013; Farahnaky and others 2013), and NFC

used as a nanofiller of the polymer matrix (Tomé and others 2013; Savadekar and others 2012). Preliminary experiments on tensile properties of the PVA-NFC films incorporated with various concentrations of glycerol and NFC were performed to determine the respective optimum concentrations for the synthesis of PVA films. Figures 4.5 and 4.6 depict data demonstrating the effect of NFC and glycerol concentrations on tensile strain (% EB) of PVA-based films of 12 ± 1mm average thickness, respectively.

Overall, PVA-based films incorporating glycerol and NFC have improved tensile properties (Virtanen and others 2014). As seen in Figure 4.6, 2.3% NFC is the optimum concentration of NFC and a concentration that was used to synthesize the films in this study. The films with less than 2.3% NFC were hard and difficult to stretch and could deform and break if higher forces were used to pull them apart. Conversely, an increase in NFC concentration to 2.3% (Figure 4.6) resulted in increased % EB for stretched films. Beyond 2.3% NFC in the films, tensile strain (% EB) of the films decreased drastically.

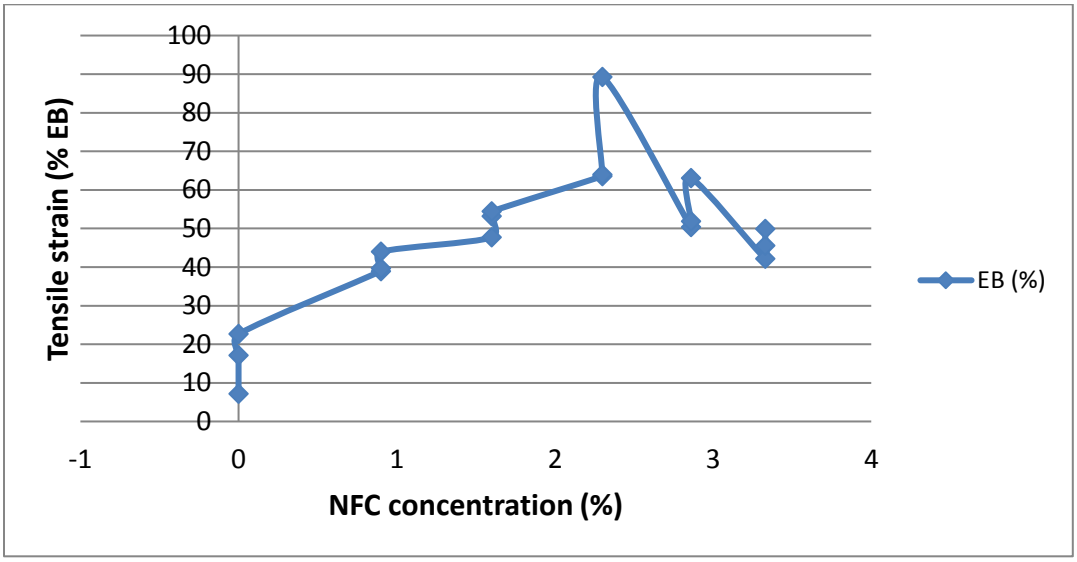

Figure 4. 6 Effect of NFC concentration on tensile strain of PVA-based films

Also, glycerol as a film plasticizer has been found to have tremendous effect on tensile characteristics of the PVA-NFC films (Farahnaky and others 2013). Figure 4.7 represents the tensile strain of the NFC-PVA films that were synthesized with varying glycerol content. As seen in Figure 4.7, increasing glycerol concentrations of the NFC-films result in increased elasticity of the NFC films, and 4.0% glycerol is an optimum concentration which makes the films more elastic. Increasing the glycerol concentration beyond 4%, however, did not affect the extensibility of the specimen but the films became oily on the surface. Thus in this study, 2.3% NFC and 4.0% glycerol were found to be optimum concentrations for synthesis of NFC-PVA films with enhanced extensibility and flexibility.

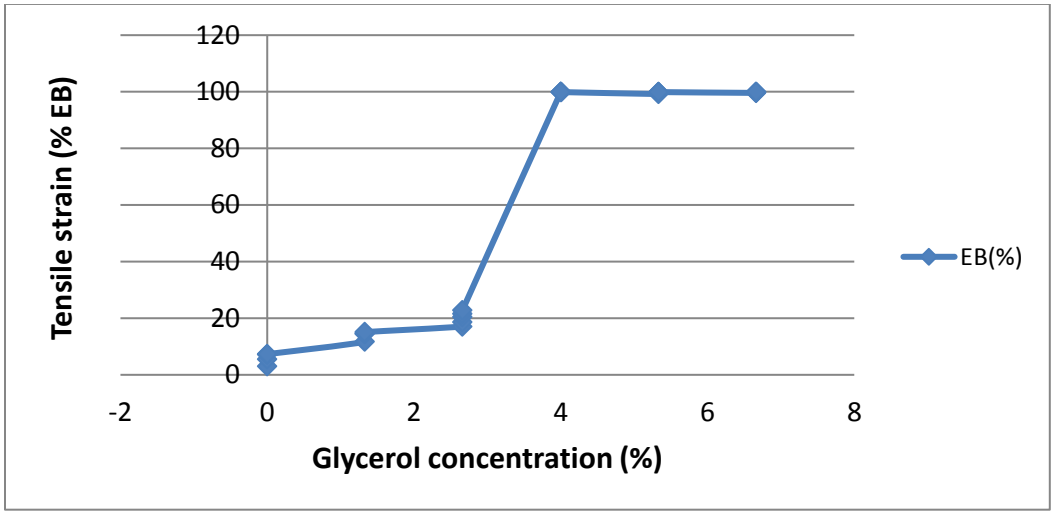

Figure 4. 7 Effect of glycerol concentration on tensile strain of PVA-based films

4.2.2 Color of the films

Color is a sensory attribute for product appearance and acceptability by the consumer (Pend and Li 2014). Table 4.2 records the averaged values for rectangular coordinates (L*, a* and b*) and color difference (ΔE) for the NFC–PVA chitosan films and those incorporating EOs.

Table 4. 2 Color and color difference of the NFC-PVA-chitosan/EO composite films

Treatment	L*	a*	b*	ΔE
PVA-NFC films	94.68a	0.14a	2.02c	0.11c
PVA-NFC chitosan	94.52a	-0.15a	2.69b	0.77b
PVA-NFC chitosan + cinnamon films	94.66a	-0.40b	3.74a	0.53a
PVA-NFC-Chitosan + clove films	94.5a	0.005a	2.64b	0.62b

Color values are expressed as means. Different letters in the same column represent significant differences between treatments and the controls ($P \leq 0.05$). As seen in Table 4.2, the color of the NFC -PVA films containing chitosan is slightly yellow (b*=2.69). With cinnamon addition to the films, yellowness significantly increased (b*=3.74) ($P \leq 0.05$), but whiteness did not significantly increase ($P > 0.05$). These data are in agreement with those of other studies on the effect of mixtures of EOs on the physical and mechanical properties of chitosan films (Peng and Li 2014). In the present

study, the data revealed that addition of cinnamon-EOs affected the color of the films. However, the color of clove-added films is significantly different ($P \leq 0.05$) from that of the controls but not significantly different ($P > 0.05$) from the color of PVA-NFC films containing chitosan. The addition of cinnamon affected the color of the films but substituting it with clove can balance the color of the films containing chitosan. Thus, it is worth noting that the color differences could be attributed to the natural color of chitosan and cinnamon as used in the film synthesis.

4.2. 3 Fourier Transform Infra-Red (FTIR) Spectroscopy

Figure 4.8 shows the FTIR spectra of glycerol (A), and PVA-NFC films (B) containing 4% glycerol, PVA-NFC films containing 1% chitosan (C), PVA-NFC films containing 1% chitosan with 0.5% cinnamon added (D), and PVA-NFC films containing 1% chitosan with 0.5% clove added (E) . As observed in that figure, the FTIR spectra of glycerol is similar to those displayed by PVA-NFC films incorporating 4% glycerol, indicating that PVA and NFC in the films were not detected with FTIR. This was evidenced by analyzing free glycerol PVA films and those prepared using NFC alone. It was found that the spectra of these polymers are quite different from those shown for the being studied films (data not shown).

Comparing the spectral peaks in Figure 4.8, it is clear that the spectral peaks for glycerol are similar to those indicated for the PVA-NFC chitosan and those containing EOs, except for the difference at their bimodal peaks. For instance, a bimodal peak is found in the region of the spectrum (2943-2888cm^{-1}) of these EOs and chitosan-added polymeric films have a peak that shifted from 2885 to 2880 cm^{-1}. Also a spectral peak shown at 1658 cm^{-1} is not present in the FTIR spectra of glycerol.

Chemical groups which are indicated by the spectral peaks of a few ingredients in the films were identified with FTIR. As seen in Figure 4.8, two major and different spectral peaks in the region between 3300 cm^{-1} and 2800 cm^{-1} are obvious. The strong absorption at 3285 cm^{-1} indicates the presence of OH-stretching and a bimodal peak at 2943-2880 cm^{-1} represents the alkyl group ($-CH_2-CH_2-$) stretch vibrations which shifted to 2880 cm^{-1}. Another important spectral peak is present in the FTIR spectrum of the films but absent in that of glycerol was localized at 1658 cm^{-1} and indicates a bending H-O-H for water.

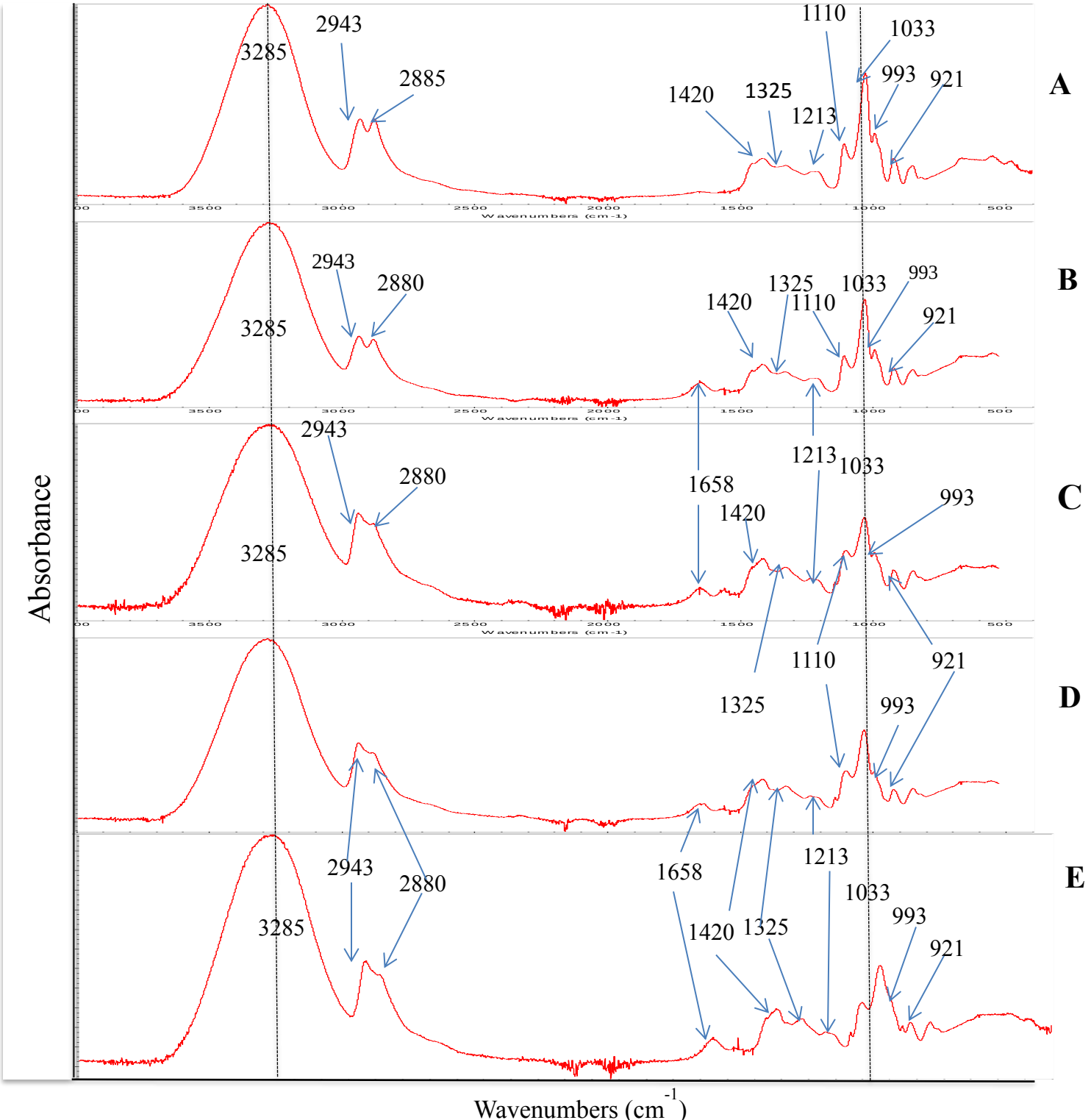

Figure 4. 8 FTIR spectra of (A): glycerol (A) and PVA-NFC films containing 4% glycerol (B)

The same fingerprint region between 1500 and 800 cm^{-1} was found to be common for FTIR spectra of glycerol and glycerol added-films. Usually, the fingerprint results from spectra displayed by similar functional groups or simultaneous chemical bond formations (Salehpour and Dubé, 2012). As seen in Figure 4.8, absorption peaks arising from COH in plane bending 1415 cm^{-1}), CH_2 bending (1213cm^{-1}), C-O-C stretch (1110 cm^{-1}), C –O stretching (1033 cm^{-1}) as primary alcohol to 1450 cm^{-1} to indicate a secondary alcohol, C-OH stretch (993 cm^{-1}) and –OH bending at 925 cm^{-1} were localized in the absorption spectrum of the films. In this study, FTIR analysis of polymeric films showed that PVA, spectral peaks indicating chemical groups of PVA, nanocellulose, chitosan and EOs were absent, as shown in Figure 4.8 and 4.9.

Table 4. 3 IR absorbance assignments for glycerol and PVA-NFC based films

Spectral region (cm^{-1})	**Absorbance assignment**
3285	O-H stretching
2943	-CH_2 symmetric stretching
2880	-CH_2 asymmetric stretching
1658	H-O-H bending
1420	C-OH in plane bending and -CH_2 Bending
1212-1325	-CH_2 wagging
1110	C-O-C stretch and C-O stretch
1023	C-O stretch
921-993	-COH stretch

However, 80% of spectral peaks of glycerol were found in the films incorporating these ingredients. In addition, the absorption peak at 1658 cm^{-1} indicates the presence of water in the films but it was found absent in the glycerol. In this study, it can be concluded that low concentration of minor film ingredients, such as EOs and strong polymer-polymer interactions due to numerous hydrogen bonding between macromolecules (cellulose, chitosan and PVA) in the films may hinder their analysis with FTIR spectroscopy.

4.2.4 Scanning electron microscopy

As indicated on Figures 4.9, 4.10, and 4.11, no significant differences were observed for the film surface morphology; all images present rough surface with long striations as entangled chain-like structures and buds which are more obvious and numerous in the EO-added films.

The surface morphology of these films can be elucidated using the theory of polymer- polymer and polymer–glycerol or EOs interactions during homogenization and emulsification (Sundaram and others 2016). In this study, it is believed that NFC and chitosan interacted in the polymer matrix (PVA) through hydrogen bonding between hydroxyl and carbonyl groups present in chitosan. As a result of these strong interactions during homogenization and inadequate emulsification, rough surface with long striations appearing like entangled chains are formed. Bud-like structures were also examined to be contributing to the roughness of the bio composite surface. These buds may be due to the presence of glycerol and EOs used in the film synthesis. Thus, total rough surface on the films indicate that the mixing was not homogeneous due to the hydrophobicity of glycerol and EOs which render them immiscible in the continuous system.

4.2.5 Energy dispersive X-ray spectroscopy (EDS)

4.2.5.1 Qualitative identification of chemical elements in the films

As seen on SEM-EDS micrographs presented on Figures 4.12, 4.14 and 4.16, seven spots on rough and smooth surfaces were selected to conduct qualitative and quantitative identification of chemical elements. The elements that were expected to be identified with this test were carbon (C), oxygen (O), and hydrogen (H) from NFC, PVA, glycerol, and EOs as the composite films were synthesized exclusively using organic ingredients. However, C and O were the only organic elements that were analyzed in all samples. Unfortunately, this method does not identify H in organic samples because organic elements (Z<11) including H and N cannot routinely be analyzed with SEM-EDS. However, Sodium (Na) was identified to be present in all kinds of the film specimens. This is because chitosan used to make the films is isolated from chitin-rich sources such as shrimp shells using sodium hydroxide (NaOH). Thus, chitosan may be contaminated with Na during chitosan synthesis.

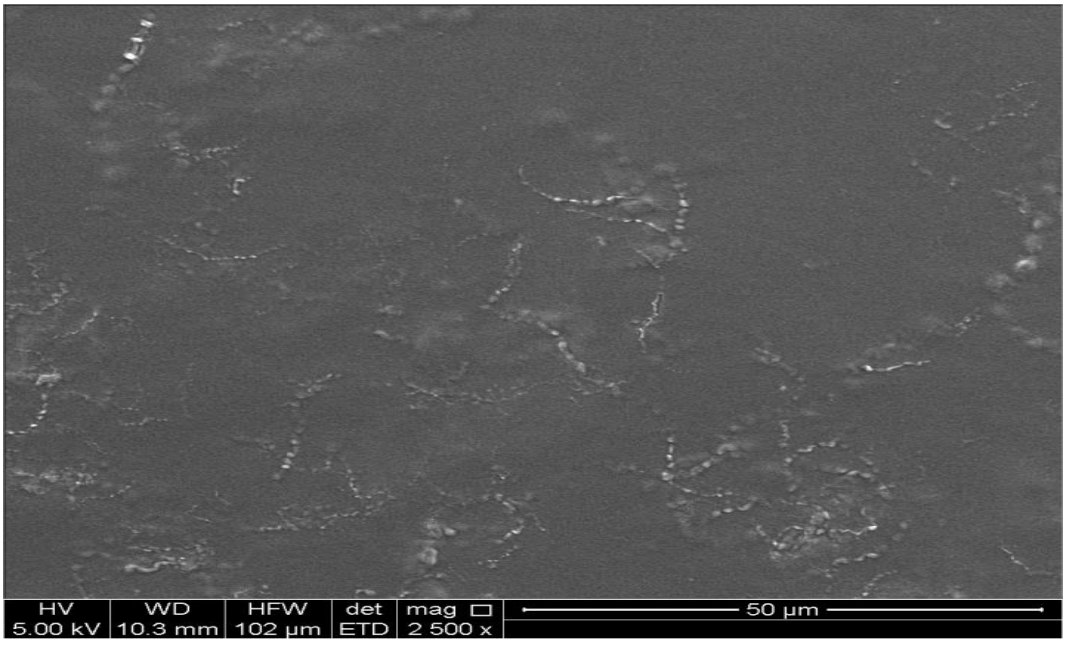

Figure 4. 9 SEM image of PVA-NFC chitosan composite films

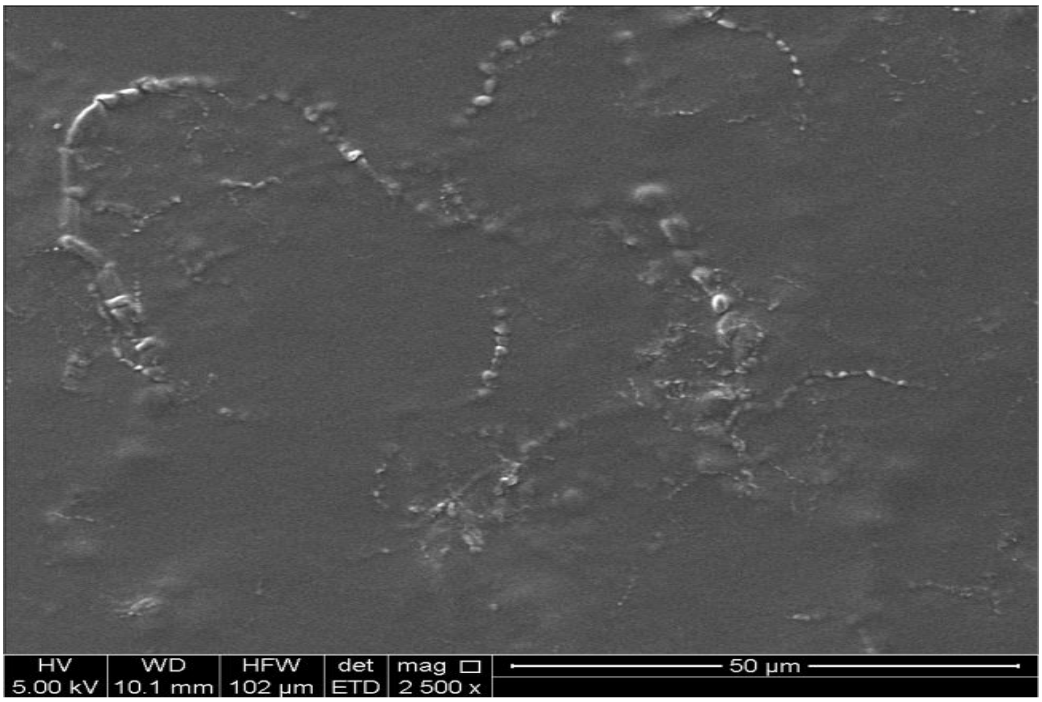

Figure 4. 10 SEM image of PVA-NFC chitosan films with cinnamon EOs

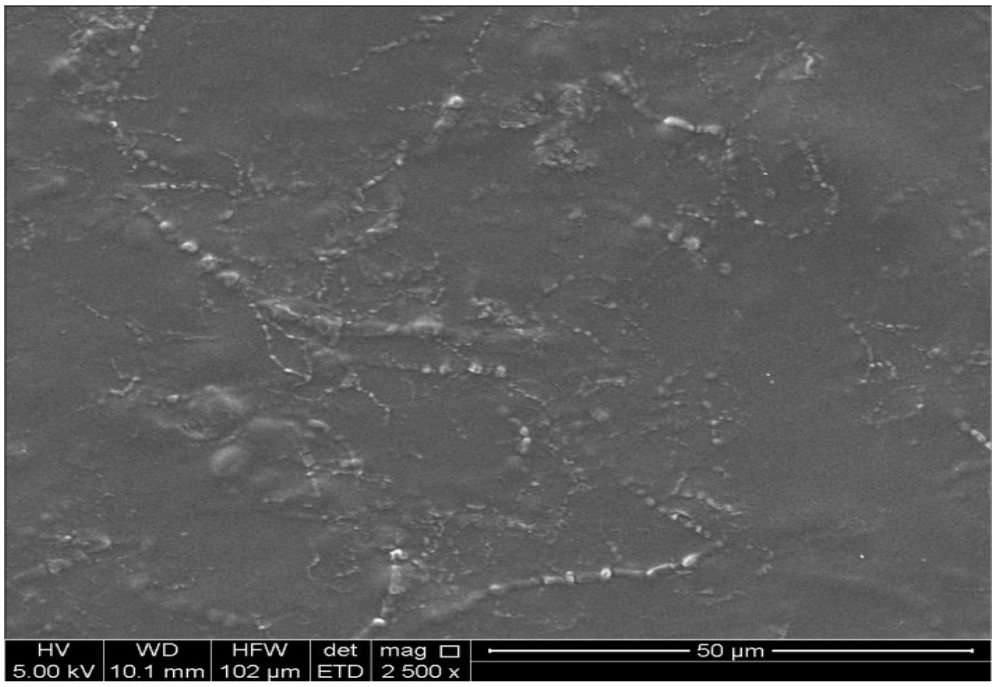

Figure 4. 11 SEM image of PVA-NFC chitosan composite films with clove EOs

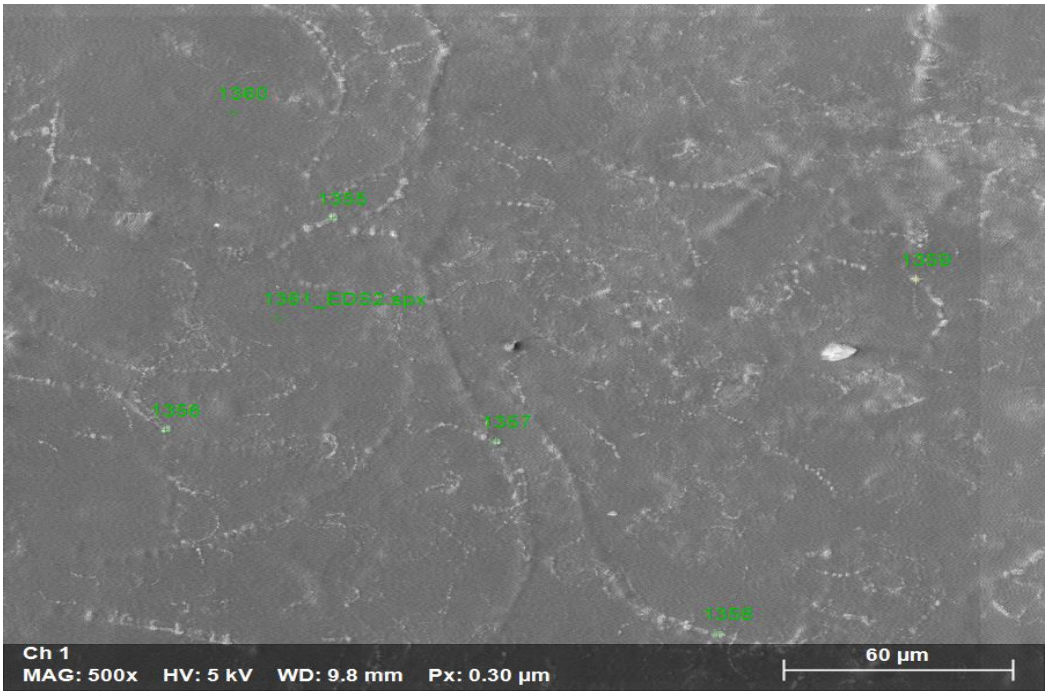

Figure 4. 12 SEM-EDS showing spotted areas on the surface of PVA-NFC chitosan composite films

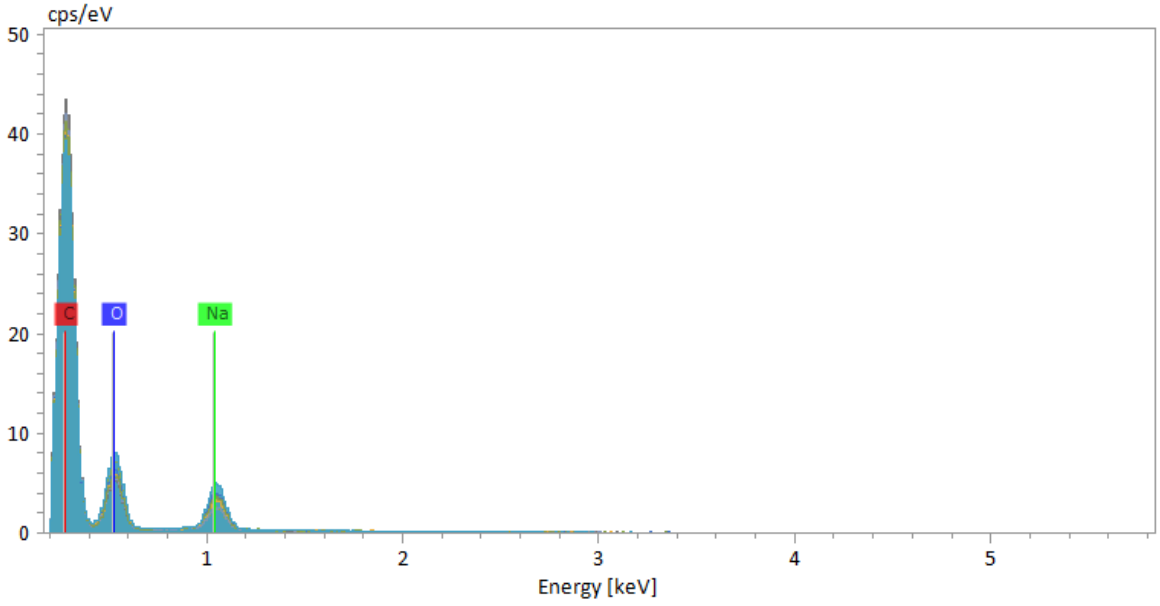

Figure 4. 13 EDS spectrum of PVA-NFC chitosan composite films

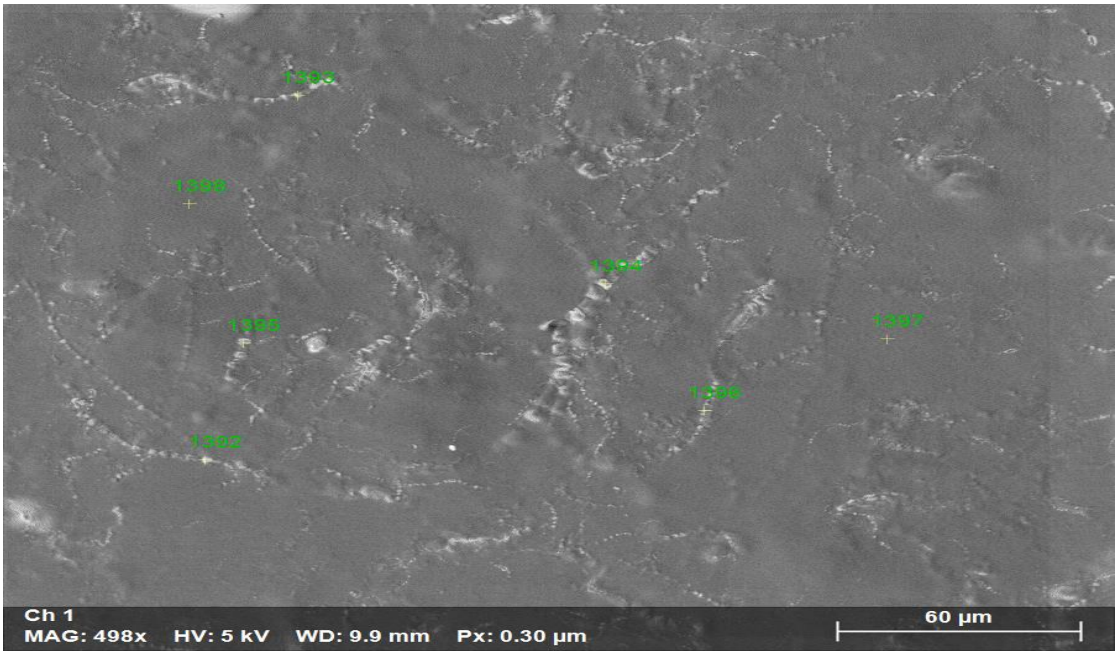

Figure 4. 14 SEM-EDS image showing spotted areas on the surface of PVA-NFC chitosan composite films incorporating cinnamon EOs

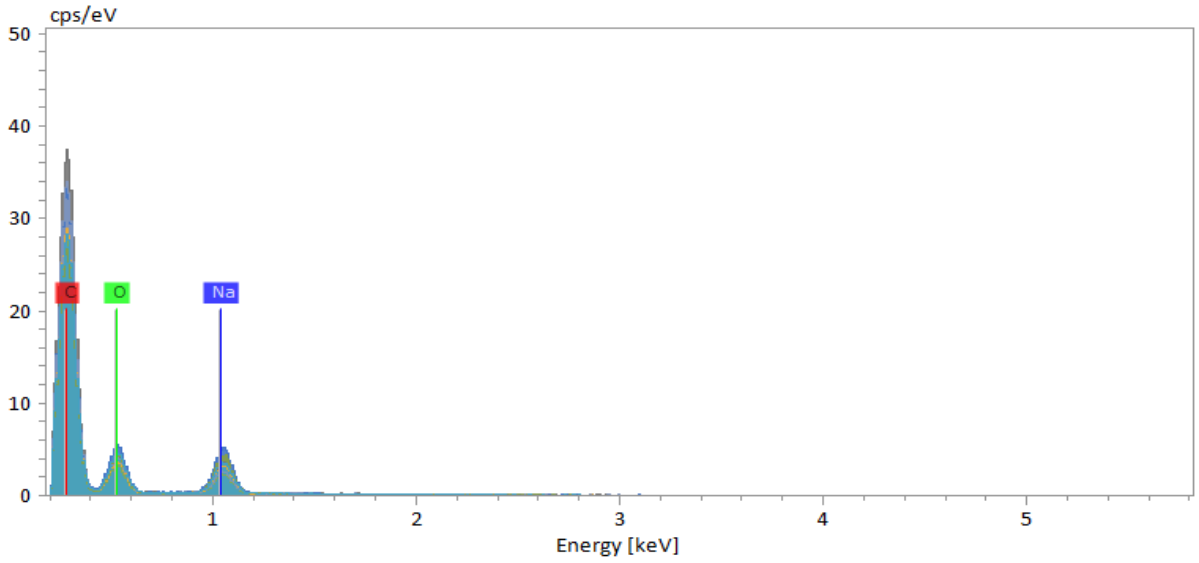

Figure 4. 15 EDS spectrum of PVA-NFC chitosan composite films incorporating cinnamon EOs

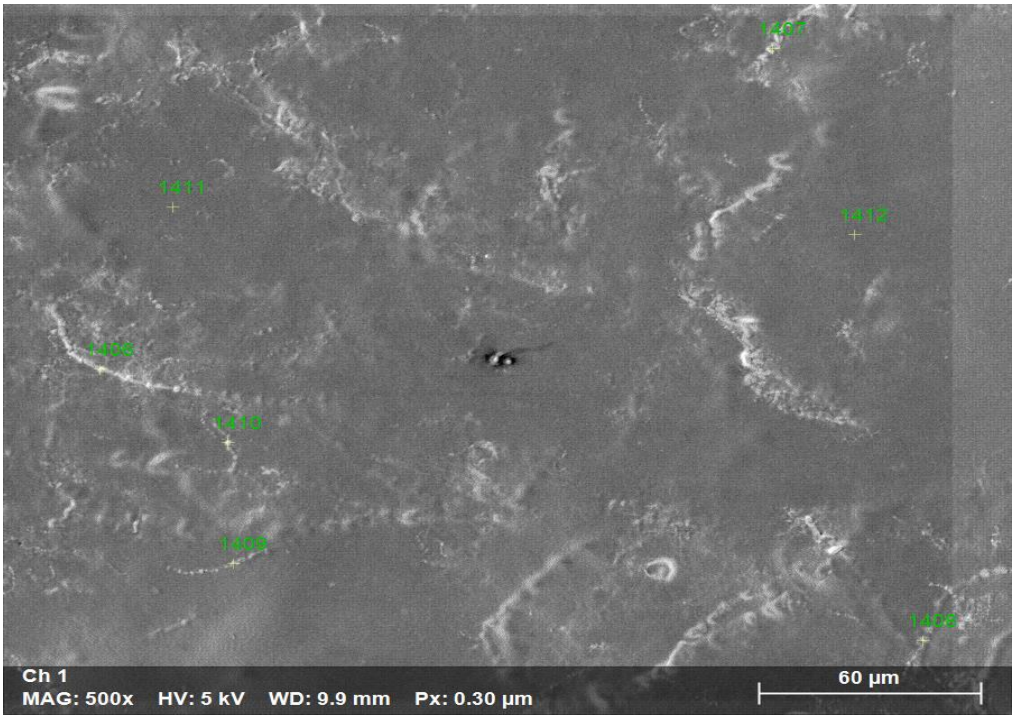

Figure 4. 16 SEM-EDS image showing spotted areas on the surface of PVA-NFC chitosan composite films incorporating clove EOs

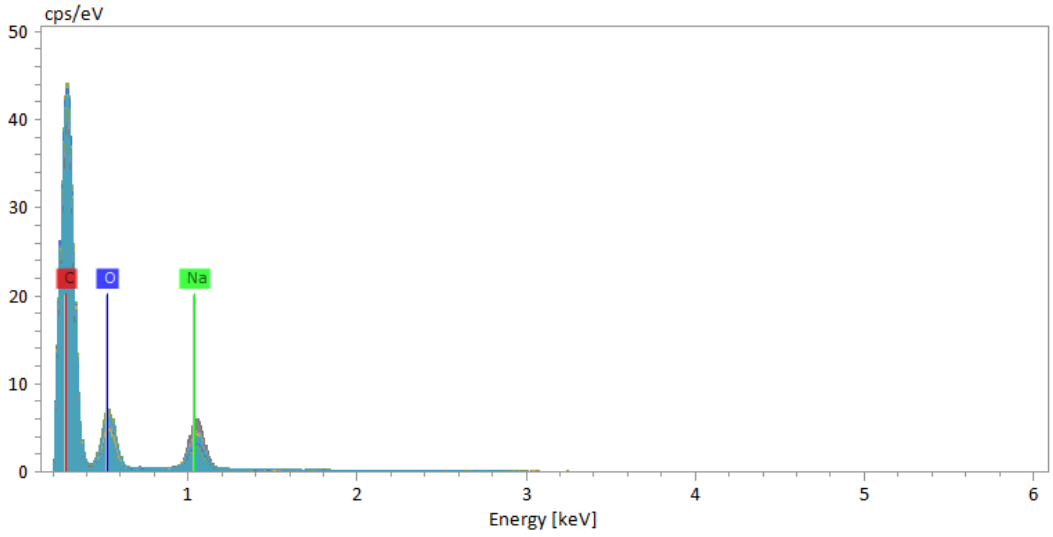

Figure 4. 17 EDS spectrum of PVA-NFC chitosan composite films incorporating clove EOs

4.2.5.2 Quantification of elements in the films

Tables 4.4, 4.5 and 4.6 below indicate relative percentages of the analyzed chemical elements in spotted areas of the film surface (Figures 10, 12 and 14). The surface analysis of films in the three treatments indicates that the atomic percentages of C are higher than those of O and Na. Comparing the data of each element as identified on different spotted areas of the film surface in all film treatments, it is obvious that there are no differences between the elemental composition of the rough and smooth surfaces of the films.

Table 4. 4 Relative atomic percentages of elements for analyzed sports on surface of PVA -NFC chitosan composite films

Spot	C	O	Na
Striation 1	85.1	12.1	2.8
Striation 2	85.1	13.4	1.5
Striation 3	81.8	13.1	5.1
Striation 4	82.8	14.3	2.8
Striation 5	83.2	14.0	2.9
Smooth 1	84.8	12.6	2.5
Smooth 2	86.2	11.3	2.5

Table 4. 5 Relative atomic percentages of elements for analyzed sports on surface of PVA-NFC chitosan films incorporating cinnamon EOs

Spot	C	O	Na
Striation 1	79.9	15.1	5.0
Striation 2	80.4	16.9	2.7
Striation 3	75.0	16.1	8.9
Striation 4	77.2	17.8	5.1
Striation 5	77.5	17.3	5.1
Smooth 1	79.7	15.8	4.5
Smooth 2	81.3	14.2	4.4

Table 4. 6 Relative atomic percentages of elements for analyzed sports on surface of PVA-NFC chitosan films incorporating clove EOs

Spot	C	O	Na
Striation 1	75.3	15.7	9.0
Striation 2	78.2	16.0	5.8
Striation 3	72.3	18.6	9.0
Striation 4	74.6	18.1	7.3
Striation 5	75.3	16.9	7.9
Smooth 1	74.8	15.9	9.3
Smooth 2	71.1	17.8	11.2

CHAPTER 5

CONCLUSIONS

5.1 Summary of the study

Innovations in the food packaging area are needed to address an environmental issue encountered with plastic packaging materials from petroleum and synthetic polymer products. Biodegradable packaging materials obtained from bio-based polymers are much needed to replace non-biodegradable packaging materials that degrade the environment. In this study, a biopolymer-based composite was successfully developed from the combination of poly (vinyl) alcohol (PVA), cellulose nanofibers (CNFs), and chitosan as biodegradable polymers.

Physical characterization of the films was performed by measuring their tensile properties with a texture analyzer (TA) and analyzing their surface. The film surface morphology was examined using Scanning electron microscopy (SEM) while the identification and quantification of chemical elements on the film surface were carried out using Energy dispersive X-ray spectroscopy (EDS).The identification of chemicals in the films by Fourier transform infrared (FTIR) spectroscopy was performed. The results of the physical tests showed that the tensile properties of the bio composite films were improved by incorporating 2.3% CNFs as a nanofiller and 4% glycerol as a plasticizer.

However, the addition of 0.5% essential oils (EOs) to the bio composite films significantly reduced the tensile stress (TS) and elongation at break (EB) values but increased the modulus of elesticity (ME). In addition, the color of the bio-composite films was significantly reduced in the films containing cinnamon EOs and or chitosan. The change in yellowness was attributed to the natural color of cinnamon and chitosan.

For morphology studies, the SEM tests revealed the presence rough and smooth surfaces of the bio composite films. The rough or striated surfaces were attributed to a strong polymer-polymer or polymer-EOs interactions due to hydrogen bonding. With EDS, the analyzed spots on smooth and striated regions of the SEM micrographs indicated that the relative atomic percentage of C was approximately five times higher than that of O, but Na was also present in trace amounts. With FTIR spectroscopy, it was shown that the spectral peaks of the biopolymers could not be detected in the bio composite films. The data showed that only glycerol peaks were present and identical in all samples. This observation was attributed to the polymer-polymer interactions which hindered the FTIR detection of composite films. EOs, however, were minor ingredients in this study and could not be detected in the films with FTIR spectroscopy.

To evaluate the antimicrobial activity of the bio composite films, an agar overlay diffusion method was used to test the chitosan and EO-added films for their inhibitory activity against various pathogenic strains. With this method, EO-added films had higher antibacterial activity than films containing chitosan alone.

In the food model, beef cuts were artificially inoculated with *E. coli* O157:H7, wrapped with the chitosan and EO-added films and stored at 4^{o}C. The results showed that after 10 days of storage, approximately 2 log reductions were achieved using chitosan or EO-added films. In the shelf-life study, *E. coli* O157:H7-free beef was wrapped with chitosan and EO-added films and stored at the above-specified conditions. It was shown that a one log reduction in the bacterial total count was achieved after 10 days of cold storage. These results in the two food model experiments suggested that chitosan and EO-

added films are capable of controlling the growth of *E. coli* O157:H7 and background flora on the beef surface.

5.2 Direction for future studies

To be able to reduce the EO-volatilization losses in the films, we recommend devising a solvent casting method. In this method, it was critical to prepare polymer-based films incorporated with cinnamon or clove EOs at higher concentrations. In this study, the amount of EOs was added in slowly to avoid the sudden aggregation phenomenon which eventually occurred when higher than 0.75% EOs were added to the being-heated and homogenized polymer solutions. It is therefore recommended to use a nano-emulsification approach to enhance the contact between EOs and polymers in solutions. With this method, the antimicrobial activity and mechanical strength as well as the optical and water barrier properties of EO-added films may be improved. Unlike films with chitosan, EO-added films used for the food model studies were observed to be moistened by the humidity of the refrigerator and or the exudates from beef.

Another challenge with EO-added films was their surface morphology studies. These films showed bud or gland-like structures indicating that improvement on emulsification is required. Thus, a proposed nano-emulsification can solve this problem.

To better understand characterization of polymer-based film with FTIR spectroscopy, a further study is needed. It was found that three polymers (chitosan, CNFs and PVA) were not detected in the films made up of these biopolymers, glycerol and EOs. Only glycerol showed up in these bio-composite films using FTIR spectroscopy. For future studies, it is recommended to increase the concentrations of these ingredients for enhanced FTIR detection method. Other techniques such as Raman and Atomic force spectroscopy can be used to characterize the bio polymer based films

REFERENCES

Aadil K, Barapatre A, Jha H Bioresour.2016. Synthesis and characterization of acacia lignin gelatin films for their possible application in food packaging. Bioprocess: 3: 27.

Ait-Quazzou A, Cherrat L,Espina L, Pagán R.2011. Antimicrobial activity of hydrophobic essential oil constituents acting alone or in combined processes of food preservation. Innov Food Sci Emerg Tech 12: 320-329.

Alemdar A, Sain M.2008. Isolation and characterization of nanofibers from agricultural residues –wheat straws and soy hulls. Bios Tech 99: 1964-1671.

Amiralian N, Annamalai PK, Memmott P, Martin DJ. 2015.Isolation of cellulose nanofibrils from Trioda purgens via different mechanical methods. Cellulose 22: 2483-2498.

Atarés L, De Jesus C, Talens P, Chiralt A. 2010. Characterization of SPI-based edible films incorporated with cinnamon or ginger essential oils.

Azevedo EP, Kumar V. 2012. Rheological, water uptake and controlled release properties of a novel- gelling aldehyde functionalized chitosan. Int J Biol Macromol 26, 63-67.

Cano A, Cháfer M, Chiralt A, González-Martínez C. 2015. Physical and antimicrobial properties of starch PVA blend films as affected by incorporation of natural antimicrobial agents. Foods 5 (3): 1-17.

Carpiné D, Dagostin JLA, Bertan LC, Mafra MR. 2005. Development and characterization of soybean protein isolate emulsion-based films with added coconut oil for olive oil packaging: barrier , mechanical and thermal properties. Food Bio Process Techn 8:1811-1823.

Castro C, Zuluaga R, Putaux JL, Caro G, Mondragon I, Gañán P. 2010. Structural characterization of bacterial cellulose produced by Glucanobacter swingsii spp. from Columbian agro-industrial wastes. J Carb Polym 84 (1): 96-102.

ChakerA, Mutjé, P, Vilar MR, Boufi S. 2014. Agriculture crops residues as a source for the production of microfibrillated cellululose with low energy demand. Cellulose Volume 21 (6):4247–4259.

Chaparo R.P, Cutierrez-Mendez N, Munoz SE, Soto JGA, Flores DC, Ochoa LH. 2015. Effect of addition of essential oils and functional extracts of clove on physical chemical properties of chitosan-based films. Int J Polym Sci: 1-6.

Chen W, Abe K, Uetani K, Yu H, Liu Y, Yano H. 2014. Individual cotton cellulose nanofibers: pretreatment and fibrillation techniques. Cellulose 23 (2): 1221-1238.

Deepa B, Abraham E, Cordeiro N, and others 2015. Utilization of various lignocellulosic biomass for the production of nanocellulose: a comparative study.
Cellulose 22(2):1075-1090.
Diplosqua R, Hoskus N, Belts G, Maurreello G. 2006. Changes in membrane fatty acid composition of microbial cells induced by addition of thymol, carvacrol, limonene, cinnamaldehyde and eugenol in the growing media. J Agri Food Chem 54 (7): 2745-2749.

Du WX, Bustillos AJA, Hua SST, McHugh TA.2011. Antimicrobial volatile essential oils in edible films for food safety.

Farahnaky A, Saberi B, Majzoobi M. 2013. Effect of glycerol on physical and mechanical properties of wheat starch edible films. J Food Text Stud 44 (3): 176-186.

Frone A, Panaitescu DM, Donescus D. 2011. Some aspects concerning the isolation of cellulose micro and nanfibers. UPB Sci Bulletin 73(2): 1-20.

Goumelon G. 2015. New World Institute analysis explores trends in global plastics consumptions and recycling.Retrieved from: http://www.worldwatch.org/global-plastic-production-rises-recycling-lags-0

Hallac BB, Ragauskas A. 2011**.** Analyzing cellulose degree of polymerization and its relevance to to cellulosic ethanol. Bio fuels Bio prod and Bioref 5(2):215 – 225.

Henriksson M, Henriksson G, Berglund LA, Lindstom T.2007**.** Environmentally friendly method for enzyme-assisted preparation of microfibrillated cellulose (MFC) nanofibers. Euro J 43 (8): 3434-3441.

Herrick FW, Casebier R.L,.Hamilton JK, Sandberg, K.R.1983. Microfibrillated cellulose: morphology and accessibility. Appl Polymer Symp 37:797-813.

Hietala M, Ämmälä A, Silvennoinen J, Liimatainen H. 2014.Fluting medium strengthened by periodate –chlorite oxidation nanofibrillated celluloses. Cellulose 23: 427:437.

Higueras L, Lopez CG, Gavara R, Hernandez MP. 2015. Reversible covalent immobilization of cinnamaldehyde on chitosan films via Schiff base formation and their application in active food packaging. 2015. Food Bio Proc Tech 8: 526- 538.

Hoeger IC,Nair SS, Ragauskas AJ, Deng Y, Rojas OJ, Zhu JY. 2013. Mechanical destruction of lignocellulose cell walls and their enzymatic saccharification. Cellulose 20 (2): 807-818.

Holley RA, Patel D. 2005. Improvement in shelf-life and safety of perishable foods by plant essential oils and smoke antimicrobials. Food Micro 22(4): 273-292.

Hu Y, Du Y, wang X, Feng T.2009.Self-aggregation of water soluble chitosan and solubilization of thymol as antimicrobila agent. J Bio Mater Res 90 (3): 874-881.

Hubbel CA, Ragauskas AJ.2010. Effect of acid –chlorite delignification on cellulose degree of polymerization. Bio Res Tech 101: 7410-7415.

Hyldgaard M, Mygind T, Mayer RL. 2012. Essential oils in food preservativation, mode of action, synergies and interaction with food matrix components. Front Micro 3 (12): 1-24.

Jiarpinijnum A, Ponchaksin P, Markino Y, Siripatrawan U. 2013. Chitosan based films containing cinnamon bark oil as an active film for food application. The society of packaging Science and Technology. Tokyo Japan.

Iwamoto S, Nakagaito A.N.2007.Micro fibrillation of pulp fibers for the processing of transparent nanocomposites. Mater Sci and Processing 89:461-466.

Iwamoto S, Nakagaito A.N, Yano H, Nogi M. 2005. Optically transparent composite reinforced with plant fibre -based nanofibers. Appl Phys 81 (6): 1109-1112.

Kazim AR. 2015.Production, optimization and characterization of cellulose produced from Pseudomonas spp. World J Experm Bio Sci 3 (2): 89-93.

Kekäläinen K, Liimatainen H, Niinimäki J. 2014. Desintegration of periodate-chlorite oxidized hard wood pulp fibres to cellulose nanofibrils: Kinetics and charge tresholds. Cellulose 21: 3691-3700.

Kim S, Jang J.2013. Effect of degree of polymerization on the mechanical properties of regenerated cellulose fibers using synthesized 1-allyl 3-methylimidazolin chloride. Fibers Polym 14 (6): 909-914.

Kolakovic R, Peltonen L **,** Laukkanen **A,** Hirvonen J, Laaksonen T. 2012. Nanofibrillar cellulose for controlled drug delivery. Eur J Pharm Biopharm 3(2): 308-315.

Kontominas MG, Badeka AV, Nerantzaki A.2006. Migration and sensory properties of plastics-based nets used as food –contact materials under ambient and high temperatures. Food Addit Contam 23(6):634-41.

Liimatainen H,Visanko M, Sirviö JA, Hormi OAO, Niinimaki J. 2015.Enhancement of the nanofibrillation of wood cellulose through sequential periodate-chlorite oxidation. Bio macro 13:1592-1597.

Liu H, Adhikari R, Guo Q, Adhikari B. 2013. Preparation and characterization of glycerol-plasticized (high amylose) starch chitosan films. J Food eng 116 (2):588-597.

López-Rubio A, Lagaron JM, Ankerfors M, Lindström T, Nordqvist D, Mattozzi A, Hedenqvist MS.2007. Enhanced film forming and thin film properties of amylopectin using micro fibrillated cellulose. Carb Polym 68 (4): 718-727.

López MA, Ruiz-Cruz S, Silva B NP, Ornalas PJJ, Ocano HVM, Rodriguez FF, Cirachavez LA, Del- Toro SCI, ShiRA k. 2015. Physicochemical and antioxidant properties of chitosan films incorporated with cinnamon oils. Int J Polym Sci, 1-8.

Mandal A, Chakrabarty D. 2011. Isolation of nanocellulose for waste sugar cane bagasse (SCB) carbohydrate polymers and its characterization. Carb Polym 86(3):1291-1299.

Mandez-Vilas A. 2011. The mode of antibacterial action of essential oils. Science against microbial pathogens: communicating current research and technological advances.

Minelli M, Baschetti MG, Ankerfors M, Lindstrom T, Siro I, Plackett D.2010.Investigation of mass transport properties of microfibrillated cellulose (MFC) films. J Membr Sci 358: 67-75.

Mingzhu P, Zhou X, Chen M.2013. Cellulose Nanowhiskers isolation and Propertiesfrom acid hydrolysis combined with high Pressure homogenization. Bio Res 8(1): 933-943.

Morais JPS, Rosa MDF, Filho MS, Nascimento LD, Nascimento DM, Cassales AR.2012. Extraction and characterization of nanocellulose structures from raw cotton linter. Carb Polym 91 (1): 229-235.

Morsy MK, Khalaf HH, Sharoba AM, El-Tanahi H.H, Cutter CN. 2014. Incorporation of essential oils in pullulan films to control food borne pathogens on meat and poultry products. J Food Sci 79(4): 675-684.

Munëz L, D'Aquino M.2012.Microbicide activity of clove essential oils (Euglia caryophyllata). Braz J Micro 43(4):1255-1260.

Nair SS, Deng Y, Ragauskas AJ. 2014. High performance green barriers based on nanocellulose. Sust Chem Proc 2:23.
Nair SS, Zhu JY, Deng Y, Ragauskas. 2014. Characterization of cellulose nanofibrillated by micro grinding. J Nanopart Res 16: 2349.

Nakagaito A.N, Nogi M, Yano H. 2010**.** Display for transparent films of natural nanofibers. MRS Bulletin 35(3): 214-215.

Nazzaro F, Fratianni F, De Martino L, Coppola R, De Feo V. 2013. Effects of essential oils on pathogenic bacteria. Pharmac 6(12): 1451-1474.

Nechyporchuk O, Pignon F, Belgacem MN. 2015. Morphological properties of nanofibrillated cellulose produced using wet grinding as an ultimate fibrillation process. J Mater Sci 50(2): 531–541.

Ojagh SM, Razei M, Razavi SH, Hosseini SMH.2010. Development and evaluation of a novel biodegradable film made from chitosan and cinnamon essential oil with low affinity toward water. Food Chem 122: 161-166.

Pääkkö M, Ankerfors M, Kosonen H, Nykänen A, Ahola S, Osterberg M, Ruokolainen J, Laine J, Larsson PT, Ikkala O, Lindström T. 2007. Enzymatic hydrolysis c ombined with mechanical shearing and high pressure homogenization for nanoscale cellulose fibrils and strong gels. Bio macro 81: 1934-1941.

Park S, Baker JO, Himmel ME, Parilla PA, Johnson DK. 2010. Cellulose crystallinity index:measurement techniques and their impact on interpreting cellulose performance. Biotech Fuel 3(10):1-10.

Pagès JM, James CE, Winterhalter M. 2008. The poison and penetrating antibiotic: a selective diffusion barrier of Gram –negative bacteria. Nat rev Micro 6: 893-903.

Peng Y, Li Y. 2014.Combined effects of two kinds of essential oils on physical, mechanical and structural properties of chitosan films. J Food Hydrocol 36: 287-293.

Radaelli M, Da Silva BP, Weidlich L, Hoehne L, FLach A, Da Costa LAMA. 2016. Antimicrobial activity of six essential oils commonly used as condiments against clostridium perfringens. Brazil J Food Micro 47(2): 424-430.

Rao LB, Kumar MM, Asha S, Sangapa Y. 2015. Mechanical and antibacterial activities of Zinc oxide incorporated into HMPC polymer nanocompsite films. RJPBCS 6(3): 767-771.

Regiel A, Iusta S, Kyziol A, Arruebo M, Santamaria J. 2012. Preparation and characterization of chitosan silver nanocomposites and their antimicrobial activities against S.aureus. Nanotech 4:
1-14.

Rodionova G, Lenes M, Erikse Ø, Gregersen Øyvind.2011.Improvement of barrier properties for packaging aplications. Cellulose 18 (1):127-134.

Scallan E, Hoestra RM, Angulo FJ, Tauxe RV, Widdowson MA, Roy SL, Jones JL,Griffin PM.2011. Food borne illness acquired in the United States –major pathogens emerging infectious diseases 17(1): 7-15.

Sharma S, Singh S, Bond J, Singh A, Rustagi A. 2014. Evaluation of antimicrobial properties of essential oils from clove and eucalyptus. Asian J Pharmar Clin Res 7: 1106-1124.

Sharma S, Zhang X, Nair SS, Ragauskas A,Zhu J,Deng Y.2014.Thermally enhanced high performance cellulose nanofibrils barrier membranes. Rsc adv 4:45136-45142.

Saito T, Kimura S, Nishiyama Y, Isogai A. 2007. Cellulose nanofillers prepared by TEMPO mediated oxidation of native cellulose. *Bio Macro*, 8 (8), 2485–2491.

Saito T, Nishiyama Y, Putaux JL, Vignon M, Isogai A. 2006. Homogeneous suspensions of individualized microfibrils from TEMPO-catalyzed oxidation of native cellulose. Bio macro 7(6),1687–1691.

Salehpour S, Dubé MA. 2012. Reaction Monitoring of glycerol step-growth polymerization using ATR-FTIR Spectroscopy. Macromol React Eng 6: 85-92.

Santos SM, Carbajo JM, Quintana E, Ibarra D, Gomez N, Ladero M, Eugenio ME, Villar JC. 2015. Characterization of purified bacterial cellulose focused on its use on paper restoration. J carb Polym 116: 173-181.

Saurabh CK, Mustapha A, Masri MM, Owalabi AF, Syakir I, Dungani R, Rwidah MT, Jawaid M, Khali HPSA. 2016.Isolation and characterization of cellulose nanofibers from giganthochlora scortechinii as reinforcement material. J Nano mater

Sanyang ML, Sapuan SM, Jawaid M, Ishak MR, Sahari J. 2015. Effect of plasticizer type and concentration on tensile stress thermal and barrier properties of biodegradable films varied on sugar palm (Arenza Pinnata) starch. Polym 7:1106- 1124.

Siripatrawan U. Harte BR.2010. Physical properties and antioxidant activity of an active film from chitosan incorporated with green tea extract. Food Colloids 24:770-775

SiripatrawanU, Noipha S.2012. Active film from chitosan incorporating green tea extract for shelf life extension of pork sausages. Food Hydrococolloids 27(1): 102–108.

Sirvio J, Kolehmaien A, Visanko M, Hormi O. 2014. Strong and self-standing oxygen barrier films from nan ocelluloses modified with regio-selective oxidative treatments. Asc Appl Mater Interfaces 6: 14384-14390

Spence KL,Venditti RA, Habibi Y, Rojas OJ, Pawlak JJ. 2010. The effect of chemical composition on microfibrillar cellulose films from wood pulps: mechanical processing and physical properties. Bio Nanotech 101(15): 5961-5968.

Soykeabkaew N, Gea S, Reynolds CT, Roohpour N, Wirjosentono B, Bilotti E, Peijs T. 2011.Investigation into structural, morphological, mechanical and thermal behaviors of bacterial cellulose after a two-step purification process. Bio Res Tech 102 (9): 9105-9110.

Sundaran J, Pant J, Goudie MJ, Mani S, Handa H. 2016.Antimicrobial and physical characterization of biodegradable nitric oxide-releasing nanocellulose-chitosan packaging membranes. J Agri Food Chem 64:5260-5266.

Svagan AJ, My A. S. Azizi Samir AS, Berglund LA.2008.Biomimetic polysaccharide monocomposite of high cellulose content and high toughness. Bio Macro 8(8): 2256-2263.

Syverud K, Stenius P.2008. Strength and barrier properties of MFC films. Cellulose 16: 75-85.

Taheri H, Samy P.2016. Effect of homogenization (micro fluidization) process parameters in mechanical production of micro and nanofibrillated cellulose and its rheological and morphological properties. Cellulose 23 (2):1221-1238.

Tejado A, Alam MN, Yang H, Antal M, Theo GM, De Ven V. 2012.Energy requirements for disintegration of cellulose fibers into cellulose nanofibers. Cellulose 19: 831-842.

Tingaut P, Zimmermann T, Lopez-Suevos F. 2010. Synthesis and Characterization of Bionanocomposites with Tunable Properties from Poly(lactic acid) and Acetylated Microfibrillated Cellulose. Bio Macro 11: 454-464.

Tomé LC, Fernandes SCM, Perez DS, Sadocco P, Silvestre AJD, Neto CP, Marrucho IM, Freire CSR. 2013.The role of nanocellulose fibers, starch and chitosan on multipolysaccharide based films. Cellulose 20 (4):1807-1818.

Turback AF. 1983. Microfibrillated cellulose, and other new cellulose product: properties, uses and other commercial potential. Symp 37: 815-827.

Ultee A, Bennink MHJ, Moezelaar R. 2002. The phenolic hydroxyl group of carvacrol is essential for action against food brone pathogene Bacillus cereus. Appl Envir Microbiol 68: 1561-1568

Vargas M, Albors A ,Chiralt A. 2011. Application of chitosan sunflower oil edible films to pork meat hamburgers. Procedia Food Sci 1: 39–43.

Virtanen S, Vartianen J, Setälä H, Tammelin T, Vuoti S. 2014. Modified nanofibrillated cellulose-polyvinyl alcohol films with improved mechanical performance. Res adv 4: 11343-11350.

Wachala R, Ramiega T, Kaczmarek A, Antczak T. 2013. Nanocellulose by enzymatic methods. Conference paper

Wang B, Sain M, Oksman K. Study of structural morphology of hemp fibers from the micro to nano scale. Appl Compos Mater 14:89-103.

Wang L, Liu F, Jiang Y, Chai Z, Li P, Cheng P, Jing H, and Leng X. 2011. Synergistic antimicrobial activities of natural essential oils with chitosan films. J Agri Food Chem 59(23):12411-12919.

Xiao S, Gao R, Gao L, Li J. 2016. Poly (vinyl) alcohol films reinforced with nanofibrillated cellulose (NFC) isolated from corn husks by high intensity ultra-sonication. Carb Polym 136:1027- 1034.

Xu C, Zhu S, Xing C, Li D, Zhu N, Zhou H. 2015.Isolation and properties of cellulose nanofibrils from coconut palm petioles by different mechanical process. Plos One 4(10): 1-11.

Yang H, Chen D, Van de Ven TGM.2015. Preparation and characterization of sterically stabilized nanocrystalline cellulose obtained by periodate oxidation of cellulose fibers. Cellulose 22: 1743-1752.

Zen M, Fevero D, Pacheco K, Grisa AMC. 2015. Preparation of microcellulose (MCC) and nano cellulose (NCC) from eucalyptus kraft spp pulp. Polym Sci 1 (7): 1-5.

Zimmermann T, Bordeanu N, Strub E. 2010. Properties of nanofibrillated cellulose from different raw materials. Carb Polym 79 (4): 1086-1093.

Zivanovic S, Chi S, Draughon AF. 2005. Antimicrobial activity of chitosan enriched with essential oils. J Food Sci 70 (1): 1-7.

VITA

Francois Xavier NAYIGIZIKI was born in the Eastern Province of Rwanda. After completing his secondary education in the 2004, Francois Xavier NAYIGIZIKI received a Rwandan government scholarship to pursue his undergraduate studies in Rwanda. In year 2009, Francois Xavier NAYIGIZIKI received his degree of Bachelor of Science in Food Science and Technology of Kigali Institute of Science & Technology (KIST). Afterwards, Francois Xavier NAYIGIZIKI desired to enhance his education through a Master's Degree program in Food Science abroad. In the year 2014, Francois Xavier NAYIGIZIKI received a US Fulbright scholarship to study in the United States. He first attended 6 months of pre-academic training at Washington State University prior to embarking on the graduate course program in Food Science at University of Missouri, Columbia in August 2014.